Table 1. Clinical findings from CTLN2 patients and controls.

Patients	Age of the nutrition survey	Age at onset of encephalopathy	Height (cm)	Weight (kg)	BMI (kg/m^2)	SLC25A13 mutation	Food fondness[1]	Alcohol drinking	Oral L-arginine (g/d)	Oral BCAA mixture (kcal/d)	Reference No.
1	51	51	160.7	60.1	23.3	II/II	+	−	—	—	12
2	45	41	173.3	64.5	21.5	V/V	+	−	10.5	—	—
3	51	51	177.2	70.4	22.4	I/V	+	−	—	—	7
4	52	52	173.0	47.5	15.9	I/II	+	−	—	—	—
5	39	38	170.0	47.0	16.3	II/XXIX	+	−	—	—	—
Mean±SD	48±6	47±7	170.8±6.2	57.9±10.4**	19.9±3.5**						
Control[2]	30–39		171.4±5.8	70.5±12.0	24.0±3.7						
	40–49		170.2±5.7	69.7±10.1	24.0±3.2						
	50–59		167.3±5.1	66.6±9.9	23.8±3.1						

**$p<0.01$.
SLC25A13 gene mutations were indicated as follows. I, 851del4 (*2*); II, IVS11+1G>A (*2*); V, IVS13+1G>A (*2*); XXIX, R588Q (*12*). [1]Food fondness for beans, milk, meat, and/or peanuts. [2]Control data were taken from the website of the Ministry for Health, Labour and Welfare in Japan (http://www.mhlw.go.jp/bunya/kenkou/eiyou08/dl/01-03.pdf). n=416 (40–49 y old).

Table 2. Laboratory data of 5 CTLN2 patients.

Patients	AST (IU/L) (12–37)	ALT (IU/L) (7–45)	Ammonia (μg/dL) (12–66)	PSTI (ng/mL) (4.6–20)	Citrulline (nmol/mL) (17.0–43.0)	Triglyceride (mg/dL) (30–150)	Fatty liver
1	36	54	29	81	95.3	66	+
2	21	24	63	56	114.3	73	+
3	52	96	64	63	408.9	300	+
4	67	77	57	240	589.5	315	+
5	19	24	236	29	292.3	60	+
Mean±SD	39±21	55±32	90±83	94±84	300.1±207.4	163±132	

The presence of fatty liver was evaluated by means of liver histology or imaging.
AST, aspartate aminotransferase; ALT, alanine aminotransferase; PSTI, pancreatic secretory trypsin inhibitor.

When she changed to her favorite meals with protein- and fat-rich and carbohydrate-low meals, only a slight increase in plasma ammonia with no increase in citrulline resulted. Thus, inappropriate nutrition can cause aggravation of symptoms and a poor clinical outcome in this disorder.

Recently, a quantitative study on food intake of young citrin-deficient subjects aged 1 to 33 y has been described (*9*). However, food intake remains unclear in CTLN2 patients, although qualitative information on food intake has been reported (*5*). While the onset age of CTLN2 varies in each patient and has been reported to range from 11 to 79 y (*10*), neuropsychological symptoms of CTLN2 begin in the third to fifth decade in most patients. Thus, in order to establish an appropriate hospital meal for citrin-deficient subjects and CTLN2 patients, quantitative characteristics of food-intake in CTLN2 patients need to be evaluated, and whether the differences in food preference exist among the age and/or between with and without CTLN2-onset needs to be defined. In the present study, food intakes in 5 CTLN2-onset patients aged 39–52 y without diet therapy were surveyed in detail.

MATERIALS AND METHODS

Patients. Five male CTLN2 patients ranging in age from 39 to 52 y (mean 48±6 y) who had been admitted to Shinshu University Hospital were examined in this study. The clinical and laboratory data of the 5 patients are shown in Tables 1 and 2, respectively. All patients suffered from repeated encephalopathic symptoms including disturbed consciousness and abnormal behavior with elevated plasma levels of ammonia and citrulline. The diagnosis of citrin deficiency was confirmed by DNA analysis of the *SLC25A13* gene (*2*, *11*, *12*). Two of the patients (patients 1 and 3) have been reported previously (*7*, *13*). In patient 1, the meal after hospitalization without diet therapy or drug therapy was surveyed. Patient 2 had begun drug therapy at the time of the survey, and his plasma ammonia was controlled by oral administration of L-arginine. His doctor had recommended that he should "not eat too many

Table 3. The nutrient intake.

Patient no.	1	2	3	4	5	CTLN2 Av.	40–49[1]
Energy (kcal/d)	1,829	2,659	2,274	2,487	2,977	2,445±430	2,188±598
% of control	84	122	104	114	136	112±20	
Protein (g/d)	101.1	100.0	103.2	129.4	132.8	113.3±16.3**	77.2±22.7
% of control	131	130	134	168	172	147±21	
PFC ratio (%)	23	15	18	21	18	19±3	14
(g/kg/d)	1.7	1.6	1.5	2.7	2.8	2.1±0.7*	1.1±0.3
Fat (g/d)	79.5	139.6	97.1	119.9	162.8	119.8±33.1**	61.1±25.5
% of control	130	228	159	196	266	196±54	
PFC ratio (%)	40	47	38	43	49	44±5**	25
Carbogytrate (g/d)	167.6	254.5	240.5	214.6	235.2	222.5±33.9	294.6±90.1
% of control	57	86	82	73	80	76±12	
PFC ratio (%)	37	38	43	36	32	37±4**	61

**$p<0.01$.

PFC ratio: protein, fat, and carbohydrate energy ratio.

[1] Age- and sex-matched Japanese male controls (2006). Data were taken from the website of the Ministry for Health, Labour and Welfare in Japan (http://www.mhlw.go.jp/bunya/kenkou/eiyou06/pdf/01-01a.pdf). $n=519$ (40–49 y old).

carbohydrates"; however, the specific quantity of carbohydrate intake was not specified. In patients 3, 4 and 5, the meal before hospitalization was surveyed, i.e., when the patients were not under a diet or drug therapy. Two patients had a low body mass index (BMI). The median weight and BMI values were lower than those of the controls (57.9±10.4 kg vs 69.7±10.1 kg, and 19.9±3.5 kg/m^2 vs 24.0±3.2 kg/m^2, respectively, $p<0.01$). Patients 1 and 2 had blood samples obtained at the time of the nutrition survey, and patients 3, 4 and 5 had blood samples obtained at admission. Three patients showed a slight elevation of serum levels of ALT and AST. Two patients had hypertriglyceridemia. Plasma ammonia was almost within normal limits in 4 patients. Plasma citrulline was high in all patients, and serum PSTI, which is a diagnostic marker of CTLN2 (*14*), was also high in all patients. Fatty liver was observed in all patients.

Evaluation of food intake. To assess daily food intakes of the patients, the Food Frequency Questionnaire (FFQg ver. 2.0 for Windows, Kenpakusha, Tokyo, Japan) was used. Intake of 18 food groups, energy, and 34 macro- and micro-nutrients was assessed by this program (*15*). The FFQ is a method of estimating intake of food groups and nutrients from the portion size and the food frequency with 1 wk as a unit. The FFQ consists of 20 question groups composed of 29 food groups and 10 kinds of cooking methods. The subjects were shown portion-sized pictures of food items and asked the quantity of each food intake and how often they consumed such foods in a week. Each subject was interviewed by a dietitian to confirm the portion size and the frequency of food eaten. The intake of each food item was estimated by multiplying the portion size by their intake frequency. Nutrient intake can also be assessed by establishing a database of compositions of the food items for target nutrients. The intake of each nutrient was calculated using the following formula for each item: (reported intake frequency per day)×(portion size in gram)×(nutrient content per 100 g)/100. The intake was then summed for all the listed food items to obtain the intake per day. Reference values from a national nutrition survey for the general Japanese population, stratified by age and sex, were previously compiled in 2006 by the Ministry for Health, Labor and Welfare in Japan (http://www.mhlw.go.jp/bunya/kenkou/eiyou06/pdf/01-01a.pdf; data only available in Japanese).

Ethics. The nutritional survey was done in the past for the purpose of the treatment, not for research. We reviewed the data of the patients who were already hospitalized many years ago; therefore we could not obtain informed consent from each patient. Although this study was not reviewed by Committee for Ethics, Shinshu University Hospital announced to all patients that their data may be used in the future with considering privacy. Those who do not want to be used for research purposes or case reports can claim an exemption.

Statistical analysis. Statistical analyses were performed using the unpaired Student's t test. A probability value of less than 0.05 was considered statistically significant.

RESULTS

Analysis of food intake

Nutritional data from the present survey including total energy, protein, fat and carbohydrate intakes, and the PFC ratios are shown in Table 3. These values were compared with those in the 40- to 49-y-old general Japanese population (values from the 2006 survey), also shown in Table 3. Total energy intake of the CTLN2 patients was 112% (2,445±430 kilocalories (kcal)) of control values. Comparing the energy ratio to total cal-

Table 4. Mineral and vitamin intake of the patients, RDA and intake of controls.

Nutrient		Intake of patients						Intake of controls[1]	RDA[2]	Sufficiency ratio of the patients for RDA (%)
		No. 1	2	3	4	5	Mean±SD			
Energy	(kcal)	1,829	2,659	2,274	2,487	2,977	2,445±430	2,188±598	2,650	92±16
Potassium	(mg)	3,017	3,687	3,508	4,072	3,498	3,557±381	2,318±827	2,000	178±19
Calcium	(mg)	628	628	794	930	1,169	830±228	487±271	650	128±35
Magnesium	(mg)	254	506	324	393	410	377±95	262±92	370	102±26
Phosphate	(mg)	1,420	1,606	1,494	1,859	2,095	1,695±279	1,067±343	1,050	161±27
Iron	(mg)	7.5	12.7	9.4	12.6	11.3	10.7±2.2	8.2±3.4	7.5	143±30
Zinc	(mg)	11	13	12	14	15	13±2	9±3	9	145±21
Copper	(mg)	1.1	2.5	1.3	1.6	1.6	1.6±0.5	1.3±0.5	0.8	201±68
Manganese	(mg)	1.8	6.0	2.7	3.1	3.5	3.4±1.6	—	4.0	85±40
Vitamin A	(μgRE)	576	461	970	1,232	812	810±308	691±1127	750	108±41
Vitamin D	(μg)	18	7	11	19	14	14±5	8±10	5	273±104
Alpha-tocopherol	(mg)	9	22	11	17	18	15±5	9±16	8	193±68
Vitamin K	(μg)	168	233	342	496	246	297±127	237±166	75	396±170
Vitamin B_1	(mg)	1.25	1.34	1.51	1.64	1.71	1.49±0.20	1.45±4.71	0.54/1,000 kcal	113±15
Vitamin B_2	(mg)	1.66	1.55	1.59	1.99	2.46	1.85±0.38	1.43±1.69	0.60/1,000 kcal	126±26
Niacin	(mg)	27	30	27	32	29	29±2	18±8	15	192±15
Vitamin B_6	(mg)	1.8	2.1	1.8	2.2	1.9	2.0±0.2	1.6±2.9	1.4	140±14
Vitamin B_{12}	(μg)	17.9	6.2	11.8	19.2	12.1	13.4±5.2	8.3±9.4	2.4	559±218
Folic acid	(μg)	280	531	438	556	359	433±116	311±179	240	180±48
Pantothenic acid	(mg)	8	9	8	9	11	9±1	6±2	6	152±22
Vitamin C	(mg)	97	95	131	160	54	107±40	90±102	100	107±40
Total dietary fiber	(g)	10.2	31.5	17.7	19.9	16.7	19.2±7.7	13.9±6.1	1 g/100 kcal	78±32
Water-soluble	(g)	2.5	4.5	4.1	4.6	2.9	3.7±1.0	3.2±2.0	—	
Water-insoluble	(g)	7.3	26.9	13.2	14.9	13.1	15.1±7.2	10.1±4.3	—	
Salt[3]	(g)	9	8	12	9	12	9±2	12±5	10	90±20
Cholesterol	(mg)	653	601	393	725	923	593±143	363±201	<750	
Fatty acid										
Total	(g)	69	126	85	105	145	96±25	—	—	
Saturated	(%E)	26	34	12	12	15	20±10	—	4.5–7	
Monounsaturated	(%E)	29	57	14	16	19	27±18	—	—	
Polyunsaturated	(%E)	14	35	7	9	10	15±11	—	—	
n-6	(g)	10	31	14	19	28	19±9	—	11	168±85
n-3	(g)	3.7	3.4	3.2	5.8	4.6	4±1	—	>2.6	160±40
n-6/*n*-3 ratio		2.6	9.1	4.2	3.3	0.2	3.9±3.3	—	4.0	

[1] Controls data were taken from the website of the Ministry for Health, Labour and Welfare in Japan (http://www.mhlw.go.jp/bunya/kenkou/eiyou06/pdf/01-01a.pdf). n=519 (40–49 y old). [2] RDA: recommend dietary allowance. [3] Salt (g)=Sodium (mg)×2.54/1,000.

ories, CTLN2 patients had significantly lower carbohydrate intake than controls (37±4% vs 61±8%, respectively, $p<0.01$). On the other hand, protein intake of CTLN2 patients was high compared to controls (113.3±16.3 g/d vs 77.2±22.7 g/d, respectively, $p<0.01$). Especially regarding daily protein intake per kg body mass, there was a significant difference between CTLN2 patients (2.1±0.7 g/kg body mass/d) and controls (1.1±0.3 g/kg body mass/d) ($p<0.01$). Patients also consumed significantly more fat (119.8±33.1 g/d) than controls (61.1±25.5 g/d) ($p<0.01$). The fat energy ratio to total calories in CTLN2 patients (44±5%) was markedly higher than in controls (25±7%) ($p<0.01$).

Intake of vitamins and minerals was compared with the recommend daily allowance (RDA) in Table 4. Mineral and vitamin intakes fulfilled the RDA in CTLN2 patients. The intake of zinc (13±2 mg) also satisfied the RDA (9 mg) in all patients. As for vitamins, all CTLN2 patients consumed 4 times more vitamin K and vitamin B_{12} than the RDA.

Analysis of intake of food groups

It has been repeatedly reported that CTLN2 patients show an aversion to carbohydrate-rich foods and a preference for protein- and fat-rich foods. To clarify the types of dietary sources of carbohydrate, protein and fat, intakes of 18 food groups were investigated (Table 5). Cereal intake of the CTLN2 patients was 309±33 g/d (590±95 kcal), which was 56% of the average cereal intakes of controls (553±197 g/d, $p<0.01$). Cereal was defined as rice, bread, noodles, and other wheat or millet products. Concerning other carbohydrate-rich foods, most patients in the present study reported only consuming a little of them, such as potatoes, fruits, sugar, and sweets. Carbohydrate-rich foods (except for cereals, mainly rice) accounted for only 50 kcal/d. As for the

Table 5. Results of the survey of daily intake of food-group in 5 patients and controls.

Patients		1	2	3	4	5	Mean±SD	Controls[1]
Cereals	(g)	278	275	321	317	355	309±33**	553±197
Potatoes	(g)	143	14	43	21	14	47±55	59±69
Fruits	(g)	21	26	43	54	0	29±21	69±118
Sugar	(g)	0.7	0.0	9.4	1.9	0.0	2.4±4.0	6.9±8.0
Sweets	(g)	0	0	36	8	0	9±16	16±41
Soybean products	(g)	10	63	50	115	65	61±38	54±73
Fish and seafood	(g)	213	57	120	226	81	139±76	86±74
Meat	(g)	149	80	194	183	216	164±53	113±81
Eggs	(g)	71	100	14	71	129	77±42*	39±38
Milk and dairy products	(g)	316	89	304	235	599	309±186**	73±119
Nuts and seeds	(g)	0.0	261.4	16.2	3.4	107.4	77.7±111.8**	1.4±4.8
Oil and fat	(g)	12	54	16	41	55	36±20**	13±10
Total vegetables	(g)	246	381	429	601	136	359±178	282±161
Light-colored	(g)	200	354	254	376	97	256±114	194±118
Deep yellow	(g)	46	27	175	225	39	102±91	88±75
Seaweed	(g)	4.3	0.7	2.9	2.1	4.3	2.9±1.5	11.7±19.5

*$p<0.05$, **$p<0.01$.

[1] Age- and sex-matched Japanese controls. Data were taken from the website of the Ministry for Health, Labour and Welfare in Japan. (http://www.mhlw.go.jp/bunya/kenkou/eiyou06/pdf/01-01a.pdf). $n=519$ (40–49 y old).

frequency of intake of potatoes and fruits, most CTLN2 patients consumed these foods 0–3 times a week. In addition, sugar intake in 4 patients was less than 2 g/d. Because 10–20 g of sugar are generally used in ordinary Japanese hospital meals, all 5 CTLN2 patients felt that the hospital meals were too sweet. Three of the 5 patients consumed sweets. Patient 3 reported consuming deep-fried food (chips) and other high fat sweets, chocolate and pudding twice a week. Patient 4 habitually ate chocolate and rice crackers once or twice a week. Patient 5 reported liking and consuming cheesecake and Yohkan (sweet jellied adzuki-bean paste) once every few months. As shown in Table 5, a significant difference was seen in intake of dairy products (especially milk, yogurts and cheeses) compared to controls (309±186 g vs 73±119 g, respectively, $p<0.01$). When compared to age-matched controls, 4 patients consumed three times more dairy products, except for patient 2, who consumed many peanuts every day. The control values for consumption of dairy products by decade were 84±139 g/d for 30- to 39-y-olds, 73±119 g/d for 40- to 49-y-olds and 77±124 g/d for 50- to 59-y-olds. Due to high intake of milk as well as other dairy products in the patients in the present study, the calcium intake was calculated to be 1.7 times greater than in the controls (Table 4). In addition, patients in the present study consumed significantly more nuts and seeds ($p<0.01$) and oil and fat ($p<0.01$) compared to controls.

Sources of fat varied among the patients. Patient 1 consumed 12 g of cooking oil, slightly less than values for the controls (13 g), but he also consumed fat from protein-rich foods that were high in fat (cod roe, saury, blue-skin fish (such as sardines and mackerels), and rib meat). Patient 2 consumed 67% of his total energy from peanuts. Patients 3 and 4 consumed fat from cooking oil and dressing (mayonnaise 50–60 g/d). Patient 5 consumed fat from cooking oil, dressing and nuts.

DISCUSSION

The present data show that diet in CTLN2 patients aged 39–52 y was unique in that they consumed low-carbohydrate and high-fat foods compared to the general Japanese population. Cereal intake was especially low in CTLN2 patients. In addition, most of the CTLN2 patients ate few fruits or sweets, although there were differences among patients surveyed. Saheki et al. surveyed daily food intakes of 18 citrin-deficient subjects aged 1–33 y, including one pre-CTLN2 patient aged 13 y (8, 9). The mean PFC ratio of the 18 citrin-deficient subjects was 19±2% : 44±5% : 37±7%, and the average carbohydrate intake of the citrin-deficient subjects was approximately half that of age- and sex-matched Japanese controls (56±14%) (9). Of particular interest in the present study was that the mean PFC ratio in CTLN2 patients (19±3% : 44±5% : 37±4%) was almost the same as that in younger citrin-deficient subjects (9).

In the research on younger citrin deficiency subjects (9), significant differences were not observed in fat intake between citrin-deficient subjects and the Japanese controls. In other words, young citrin deficient subjects had a fat intake within 1 standard deviation of Japanese control subjects. Commonly, fat intake gradually declines with age in the general Japanese population. According to the 2006 survey (http://www.mhlw.go.jp/bunya/kenkou/eiyou08/dl/01-05.pdf), the median (50 percentile) of the fat energy ratio was 30% in 1- to 29-y-olds. However, this value was less than 25% in controls >30 y of age. The percentage of people with a fat intake of more than 35% of total energy was only 9% in 40- to 49-y-old men, and 4.3% in 50- to 59-y-old men. In the

present study, the fat energy ratio of CTLN2 was more than 38%, and fat intakes were higher than in age- and sex-matched Japanese controls. Patients 2 and 5 had fat intakes more than 3 standard deviations from that of controls, and patient 4 was more than 2 standard deviations from the controls. Therefore, a high-fat diet was a characteristic in older CTLN2 patients than younger citrin-deficient subjects. In the 2006 survey, meat, oil and fat intakes peaked in 15- to 19-y-olds (male intake: 156.6 g/d of meat, 16.4 g/d of oil and fat) and the intakes decreased to less than 77% of the peak value in 40–49-y-olds. On the other hand, intake of soybean products, fish and vegetables increased with age. The present results, however, indicate that CTLN2 patients continued to consume high-fat meals regardless of age, although the source of the fat varied among patients. The fat intake of the present CTLN2 patients relative to the average values for controls was 196% (Table 3), suggesting that fat was the main energy source in CTLN2 patients.

A significant difference was also seen in intake of dairy products ($p<0.01$). In the 2006 survey, the peak age of intake of dairy products was observed in 7- to 14-y-olds (359.1 g/d) and decreased with age. In 40- to 49-y-olds, it was only 72.8 g/d. On the other hand, the present CTLN2 patients consumed three times more dairy products compared to control subjects of the same age. While the precise reason why CTLN2 patients prefer dairy products remains obscure, their preference may be associated with low carbohydrate and high fat content (the PFC ratio of milk is 20% : 50% : 30%).

Together with previous data reported by Saheki et al. (9), the present results may indicate that aversion to carbohydrates is fundamentally seen regardless of a patient's age. Therefore, even in older patients, a high-fat and high-protein diet seems to be required to compensate for lack of energy due to aversion to carbohydrates.

Carbohydrate aversion in citrin deficiency is thought to be quite unique in contrast to the protein aversion in other urea cycle enzyme deficiencies (9). In citrin deficiency, carbohydrate metabolism facilitates accumulation of cytosolic NADH in hepatocytes, resulting in inhibition of ureagenesis by limitation of the supply of Asp for the urea cycle (3, 4). Previous data have suggested that the toxicity of a high carbohydrate intake (8), and indeed, intravenous infusion of a high glucose solution or the administration of a glycerol solution, result in severe hyperammonemia or rapid deterioration of encephalopathy leading to death in many CTLN2 patients (6, 16). A CTLN2 patient (patient 3 in the present study) who had a rapid deterioration after consuming a conventional low-protein diet for hepatic encephalopathy, in which the energy ratio of carbohydrates in total diet energy was around 75%, has been previously reported (7). It has also been found that oral sucrose administration exacerbated hyperammonemia in citrin/mitochondrial glycerol 3-phosphate dehydrogenase double knockout mice, an animal model of human citrin deficiency (17). Therefore, high carbohydrate intake can deteriorate hepatic encephalopathy in CTLN2 patients. The efficacy of a carbohydrate-restricted diet in citrin deficiency patients has been described in a few patients (7, 18, 19). In patient 3 in the present study, induction of a low-carbohydrate diet (PFC ratio 15% : 40% : 45%) was therapeutically effective against encephalopathy (7).

In conclusion, CTLN2 patients in this study consumed low-carbohydrate, high-fat, and high-protein diets, similar to younger individuals with citrin deficiency, and therefore, it appears that the PFC ratio of citrin-deficient subjects is not influenced by age or CTLN2-onset. Carbohydrates were strictly adjusted by total intake of cereals in our patients. A conventional hospital diet for hyperammonemia may be risky in treatment of CTLN2 patients because of its high carbohydrate content. A low-carbohydrate and high-fat diet is recommended for patients with CTLN2 and from results of the nutrition survey in the present study and data reported previously (7–9, 19), 1,720-kcal meals have been recently served with 130 g boiled rice and 70 g protein (PFC ratio15% : 45% : 40%) as a basic hospital diet for CTLN2 patients in our hospital. However, since our data was obtained from a small number of patients, further study may be needed to confirm our results and to establish a more appropriate diet for CTLN2 patients.

Acknowledgments

This study was supported in part by Grants-in-Aid for Scientific Research (B) (No 19390096 to KK), Asia-Africa Science Platform Program from the Japan Society for the Promotion of Science and grants of the citrin working group from the Ministry of Health, Labor and Welfare of Japan.

REFERENCES

1) Palmieri L, Pardo B, Lasorsa FM, del Arco A, Kobayashi K, Iijima M, Runswick MJ, Walker JE, Saheki T, Satrústegui J, Palmieri F. 2001. Citrin and aralar1 are Ca^{2+}-stimulated aspartate/glutamate transporters in mitochondria. *EMBO J* **20**: 5060–5069.

2) Kobayashi K, Sinasac DS, Iijima M, Boright AP, Begum L, Lee JR, Yasuda T, Ikeda S, Hirano R, Terazono H, Crackower MA, Kondo I, Tsui LC, Scherer SW, Saheki T. 1999. The gene mutated in adult-onset type II citrullinaemia encodes a putative mitochondrial carrier protein. *Nat Genet* **22**: 159–163.

3) Saheki T, Kobayashi K, Iijima M, Moriyama M, Yazaki M, Takei Y, Ikeda S. 2005. Metabolic derangements in deficiency of citrin, a liver-type mitochondrial aspartate-glutamate carrier. *Hepatol Res* **33**: 181–184.

4) Saheki T, Kobayashi K. 2002. Mitochondrial aspartate glutamate carrier (citrin) deficiency as the cause of adult-onset type II citrullinemia (CTLN2) and idiopathic neonatal hepatitis. *J Hum Genet* **47**: 333–341.

5) Kobayashi K, Saheki T. 2004. Molecular basis of citrin deficiency. *Seikagaku* **76**: 1543–1559 (in Japanese).

6) Takahashi H, Kagawa T, Kobayashi K, Hirabayashi H, Yui M, Begum L, Mine T, Takagi S, Saheki T, Shinohara Y. 2006. A case of adult-onset type II citrullinemia—deterioration of clinical course after infusion of hyperos-

motic and high sugar solutions. *Med Sci Monit* **12**: CS13–15.
7) Fukushima K, Yazaki M, Nakamura M, Tanaka N, Kobayashi K, Saheki T, Takei H, Ikeda S. 2010. Conventional diet therapy for hyperammonemia is risky in treatment of hepatic encephalopathy associated with citrin deficiency. *Intern Med* **49**: 1–20.
8) Saheki T, Inoue K, Tushima A, Mutoh K, Kobayashi K. 2010. Citrin deficiency and current treatment concepts. *Mol Genet Metab* **100**: S59–S64.
9) Saheki T, Kobayashi K, Terashi M, Ohura T, Yanagawa Y, Okano Y, Hattori T, Fujimoto H, Mutoh K, Kizaki Z, Inui A. 2008. Reduced carbohydrate intake in citrin-deficient subjects. *J Inherit Metab Dis* **31**: 386–394.
10) Yasuda T, Yamaguchi N, Kobayashi K, Nishi I, Horinouchi H, Jalil MA, Li MX, Ushikai M, Iijima M, Kondo I, Saheki T. 2000. Identification of two novel mutations in the *SLC25A13* gene and detection of seven mutations in 102 patients with adult-onset type II citrullinemia. *Hum Genet* **107**: 537–545.
11) Yamaguchi N, Kobayashi K, Yasuda T, Nishi I, Iijima M, Nakagawa M, Osame M, Kondo I, Saheki T. 2002. Screening of *SLC25A13* mutations in early and late onset patients with citrin deficiency and in the Japanese population: Identification of two novel mutations and establishment of multiple DNA diagnosis methods for nine mutations. *Hum Mutat* **19**: 122–130.
12) Tabata A, Sheng JS, Ushikai M, Song YZ, Gao HZ, Lu YB, Okumura F, Iijima M, Mutoh K, Kishida S, Saheki T, Kobayashi K. 2008. Identification of 13 novel mutations including a retrotransposal insertion in *SLC25A13* gene and frequency of 30 mutations found in patients with citrin deficiency. *J Hum Genet* **53**: 534–545.
13) Soeda J, Yazaki M, Nakata T, Miwa S, Ikeda S, Hosoda W, Iijima M, Kobayashi K, Saheki T, Kojiro M, Miyagawa S. 2008. Primary liver carcinoma exhibiting dual hepatocellular-biliary epithelial differentiations associated with citrin deficiency: a case report and review of the literature. *J Clin Gastroenterol* **42**: 855–860.
14) Kobayashi K, Horiuchi M, Saheki T. 1997. Pancreatic secretory trypsin inhibitor as a diagnostic marker for adult-onset type II citrullinemia. *Hepatology* **25**: 1160–1165.
15) Takahashi K, Yoshimura Y, Kaimoto T, Kunii D, Komatsu T, Yamamoto S. 2001. Validation of a Food Frequency Questionnaire Based on Food Groups for Estimating Individual Nutrient Intake. *Jpn J Nutr Diet* **59**: 221–232 (in Japanese).
16) Yazaki M, Takei Y, Kobayashi K, Saheki T, Ikeda S. 2005. Risk of worsened encephalopathy after intravenous glycerol therapy in patients with adult-onset type II citrullinemia (CTLN2). *Intern Med* **44**: 188–195.
17) Saheki T, Iijima M, Li MX, Kobayashi K, Horiuchi M, Ushikai M, Okumura F, Meng XJ, Inoue I, Tajima A, Moriyama M, Eto K, Kadowaki T, Sinasac DS, Tsui LC, Tsuji M, Okano A, Kobayashi T. 2007. Citrin/mitochondrial glycerol 3-phosphate doubleknockout mice recapitulate features of human citrin deficiency. *J Biol Chem* **282**: 25041–25052.
18) Imamura Y, Kobayashi K, Shibatou T, Aburada S, Tahara K, Kubozono O, Saheki T. 2003. Effectiveness of carbohydrate-restricted diet and arginine granules therapy for adult-onset type II citrullinemia: a case report of siblings showing homozygous *SLC25A13* mutation with and without the disease. *Hepatol Res* **26**: 68–72.
19) Dimmock D, Kobayashi K, Iijima M, Tabata A, Wong LJ, Saheki T, Lee B, Scaglia F. 2007. Citrin deficiency: a novel cause of failure to thrive that responds to a high protein, low carbohydrate diet. *Pediatrics* **119**: 773–777.

Journal of Neuroscience Research

Journal of Neuroscience Research 88:1009–1016 (2010)

Low Levels of Citrin (*SLC25A13*) Expression in Adult Mouse Brain Restricted to Neuronal Clusters

Laura Contreras,[1,2] Almudena Urbieta,[1] Keiko Kobayashi,[3] Takeyori Saheki,[4] and Jorgina Satrústegui[1,2]*

[1]Departamento de Biología Molecular, Centro de Biología Molecular Severo Ochoa CSIC-UAM, Universidad Autónoma de Madrid, Madrid, Spain
[2]CIBER de Enfermedades Raras (CIBERER), Madrid, Spain
[3]Department of Molecular Metabolism and Biochemical Genetics, Kagoshima University Graduate School of Medical and Dental Sciences, Kagoshima, Japan
[4]Institute for Health Sciences, Tokushima Bunri University, Yamashiro-cho, Tokushima, Japan

The mitochondrial aspartate-glutamate carriers (AGC) aralar (*SLC25A12*) and citrin (*SLC25A13*) are components of the malate aspartate shuttle (MAS), a major intracellular pathway to transfer reducing equivalents from NADH to the mitochondrial matrix. Aralar is the main AGC isoform present in the adult brain, and it is expressed mainly in neurons. To search for the other AGC isoform, citrin, in brain glial cells, we used a citrin knockout mouse in which the lacZ gene was inserted into the citrin locus as reporter gene. In agreement with the low citrin levels known to be present in the adult mouse brain, β-galactosidase expression was very low. Surprisingly, unlike the case with astroglial cultures that express citrin, no β-galactosidase was found in brain glial cells. It was confined to neuronal cells within discrete neuronal clusters. Double-immunolabelling experiments showed that β-galactosidase colocalized not with glial cell markers but with the pan-neuronal marker NeuN. The deep cerebellar nuclei and a few midbrain nuclei (reticular tegmental pontine nuclei; magnocellular red nuclei) were the regions where β-galactosidase expression was highest, and it was up-regulated in fasted mice, as was also the case for liver β-galactosidase. The results support the notion that glial cells have much lower AGC levels and MAS activity than neurons.

Key words: mitochondrial aspartate-glutamate carrier; citrin; aralar; redox shuttle; neuron; cerebellum; fasting; OmniBank

The malate aspartate shuttle (MAS) is, together with the glycerol-3-phosphate shuttle, a major intracellular pathway to transfer glycolytic redox equivalents to the mitochondrial matrix (Dawson, 1979; McKenna et al., 2006). MAS is composed of two enzymes located in the cytosol and mitochondrial matrix compartments (aspartate transaminase and malate dehydrogenase) and of two transporters belonging to the mitochondrial carrier superfamily (Walker and Runswick, 1993). The oxoglutarate carrier (OGC) transports malate in exchange for α-ketoglutarate (electroneutral and reversible; Indiveri et al., 1991; Smith and Walker, 2003), whereas the aspartate-glutamate carrier (AGC) cotransports cytosolic glutamate (plus a proton) against mitochondrial aspartate (for review see Satrustegui et al., 2007). In mammals, two isoforms of the AGC exist: aralar, also named *aralar1* (*SLC25A12*) and citrin (*SLC25A13*; del Arco and Satrustegui, 1998; Kobayashi et al., 1999; del Arco et al., 2000). Both have Ca^{2+}-binding motifs (EF-hands) in their N-terminal halves facing the intermembrane space (Palmieri et al., 2001). This allows the activation of AGCs and MAS in response to cytosolic calcium signals that do not reach the mitochondrial matrix (Pardo et al., 2006; Contreras et al., 2007; Marmol et al., 2009). Ca^{2+} activation of glutamate transport along the AGC is also responsible for calcium stimulation of respiration in brain mitochondria using glutamate and malate as respiratory substrates (Gellerich et al., 2008). The two AGC isoforms differ mainly in terms of calcium sensitivity (Con-

Laura Contreras's current addresss is Department of Biomedical Sciences; University of Padua; Viale Giuseppe Colombo 3, 35121 Padua, Italy

Contract grant sponsor: Ministerio de Educación y Ciencia; Contract grant number: BFU2005-C02-01; Contract grant number: BFU2008-04084/BMC; Contract grant sponsor: Comunidad de Madrid; Contract grant number: S-GEN-0269-2006 MITOLAB-CM; Contract grant sponsor: European Union; Contract grant number: LSHM-CT-2006-518153; Contract grant sponsor: Fundación Ramón Areces (to the Centro de Biología Molecular Severo Ochoa).

*Correspondence to: Jorgina Satrústegui, Departamento de Biología Molecular, Centro de Biología Molecular "Severo Ochoa" CSIC-UAM, c/ Nicolás Cabrera 1, Campus Cantoblanco, 28049-Madrid, Spain.
E-mail: jsatrustegui@cbm.uam.es

Received 8 July 2009; Revised 1 September 2009; Accepted 3 September 2009

Published online 11 November 2009 in Wiley InterScience (www.interscience.wiley.com). DOI: 10.1002/jnr.22283

treras et al., 2007) and tissular distribution (del Arco et al., 2000, 2002; Begum et al., 2002). During embryonic development, they share an overlapping pattern, but citrin becomes the main AGC isoform in the adult liver, whereas aralar is the main isoform in skeletal muscle and brain cells. Other adult tissues such as heart and kidney express both isoforms (del Arco et al., 2000, 2002; Begum et al., 2002; Contreras et al., 2007). In aralar$^{-/-}$ mice, mitochondria from brain or muscle have essentially no MAS activity, and respiration with glutamate and malate as substrates is extremely reduced (Jalil et al., 2005), in agreement with the lack of the major AGC isoform present in these tissues. A strong reduction in ATP production by muscle mitochondria during respiration with glutamate and malate has also been described in a 3-year-old child with a homozygous missense mutation in aralar (Wibom et al., 2009). Within the brain, aralar is preferentially expressed in neurons, as shown by immunolabelling and in situ hybridization data and by mRNA levels in acutely isolated brain cells (Ramos et al., 2003; Xu et al., 2007; Berkich et al., 2007; Cahoy et al., 2008), but there are conflicting results regarding this issue (Lovatt et al., 2007). A preferential expression of aralar in neurons is consistent with higher levels of aralar in total than in synaptosomal-free mitochondrial brain fractions (Berkich et al., 2007) and higher MAS activity in neuronal than in astrocyte cultures (Ramos et al., 2003), with aralar being one of the more enriched proteins during differentiation of P19 cells to a neuronal phenotype (Watkins et al., 2008).

Paradoxically, although neither citrin mRNA nor protein was found in the adult rodent brain (Ramos et al., 2003), both are expressed in glial cultures (Ramos et al., 2003) and have been detected by in situ hybridization at low levels in the adult spinal cord (www.brain-map.org). These results opened up the possibility that citrin could be present in the brain glial cells and thus compensate for their low levels of aralar. This is an important and controversial issue, insofar as redox shuttle levels in astrocytes are critical to explain the extent to which dynamic changes in glucose utilization are accompanied by the transfer of redox equivalents to and pyruvate oxidation in mitochondria or by regeneration of NAD^+ in the cytosol and lactate production. A preferential production of lactate from glucose by astrocytes is central to the astrocyte–neuron lactate shuttle hypothesis (ANLSH), according to which astrocytic lactate is transferred to neurons for oxidation (Pellerin et al., 2007).

In the present work, we have aimed to clarify whether citrin is expressed in the brain and, if so, whether its expression is glial. To do this, we have used citrin-deficient mice (Contreras et al., 2007), which have β-galactosidase (β-gal) as reporter gene in the insertion cassette. In these β-gal knock-in mice, expression of the β-gal reporter is controlled by all the endogenous regulatory elements of the *SLC25A13* gene, so β-gal will be expressed instead of citrin and will respond to the same cues. This β-gal knock-in strategy has been proved to be a powerful tool with which to study the localized gene expression in other gene knockout animals (Gow et al., 1992; de Leeuw et al., 2006; Couegnas et al., 2007; Karavanova et al., 2007). Surprisingly, the results obtained clearly show that citrin is expressed only in neurons.

MATERIALS AND METHODS

Animals

Three-month-old citrin$^{-/-}$ and citrin$^{+/+}$ (Contreras et al., 2007) mice were housed with a 12-hr light cycle and fed ad libitum on standard chow. All animal procedures were approved by European guidelines. Unless otherwise stated, reagents were purchased from Sigma-Aldrich (Tres Cantos, Spain).

Animals were anesthetized with chloral hydrate (0.5 mg/g body weight) and perfused transcardially with saline buffer (0.9% NaCl in phosphate buffer) and then with 4% formaldehyde in phosphate buffer (formalin fixative). Brains were carefully removed, postfixed overnight in formalin (4°C), and transferred into sucrose (30% in phosphate buffer). Once the brains had sunk to the bottom of the container, they were embedded in OCT compound (Tissue-Tek; Sakura Finetek Europe B.V., Zoeterwoude, The Netherlands), frozen on dry ice, and cut into 12 series of 30-μm coronal sections with a criotome (free-floating sections). Sections were kept in a cryoprotectant medium (25% glycerol, 25% ethylene glycol in 50 mM phosphate buffer) and stored at –20°C until processing (Couegnas et al., 2007).

Citrin Localization: X-gal Assay and Immunohistochemistry

For the detection of β-galactosidase expression, the X-gal detecting kit (Stratagene, La Jolla, CA) was used. Briefly, sections were tempered and washed free of cryoprotectant media with PBS before incubating them in X-gal staining solution for 3 days (30°C), to allow for the blue product deposition in the tissue. When appropriate, sections were washed to remove excess substrate before beginning the inmunohistochemistry procedure. After quenching endogenous peroxidase (30 min incubation in 3% H_2O_2, 10% methanol, PBS), sections were blocked in 10% horse serum + 0.5% Triton X-100 (2 hr) and incubated with the following antibodies overnight (at 4°C): GFAP (1/2,000; Sigma, St. Louis, MO; clone GA5 No. G3893) as glial marker or NeuN (1/500; Chemicon, Temecula, CA; MAB377) as neuronal marker. The secondary antibody used was BA2001 (1/250; Vector, Burlingame, CA), and the signal was amplified with Vectastain ABC kit (Vector) before diaminobenzidine tetrahydrochloride (DAB) detection. After dehydratation, slides were mounted with DPX (BDH, VWR International Ltd., Poole, Unitede Kingdom) for analysis.

For inmunofluorescence assays, sections were treated with $NaBH_4$ to quench endogenous autofluorescence before blocking. The following primary antibodies, together with appropriate secondary antibodies, were employed: β-gal (1/500, 5prime-3prime Inc., Boulder, CO), NeuN (1/500), GFAP (1/2,000), and MAP-2 (1/500; Sigma M4403). Sec-

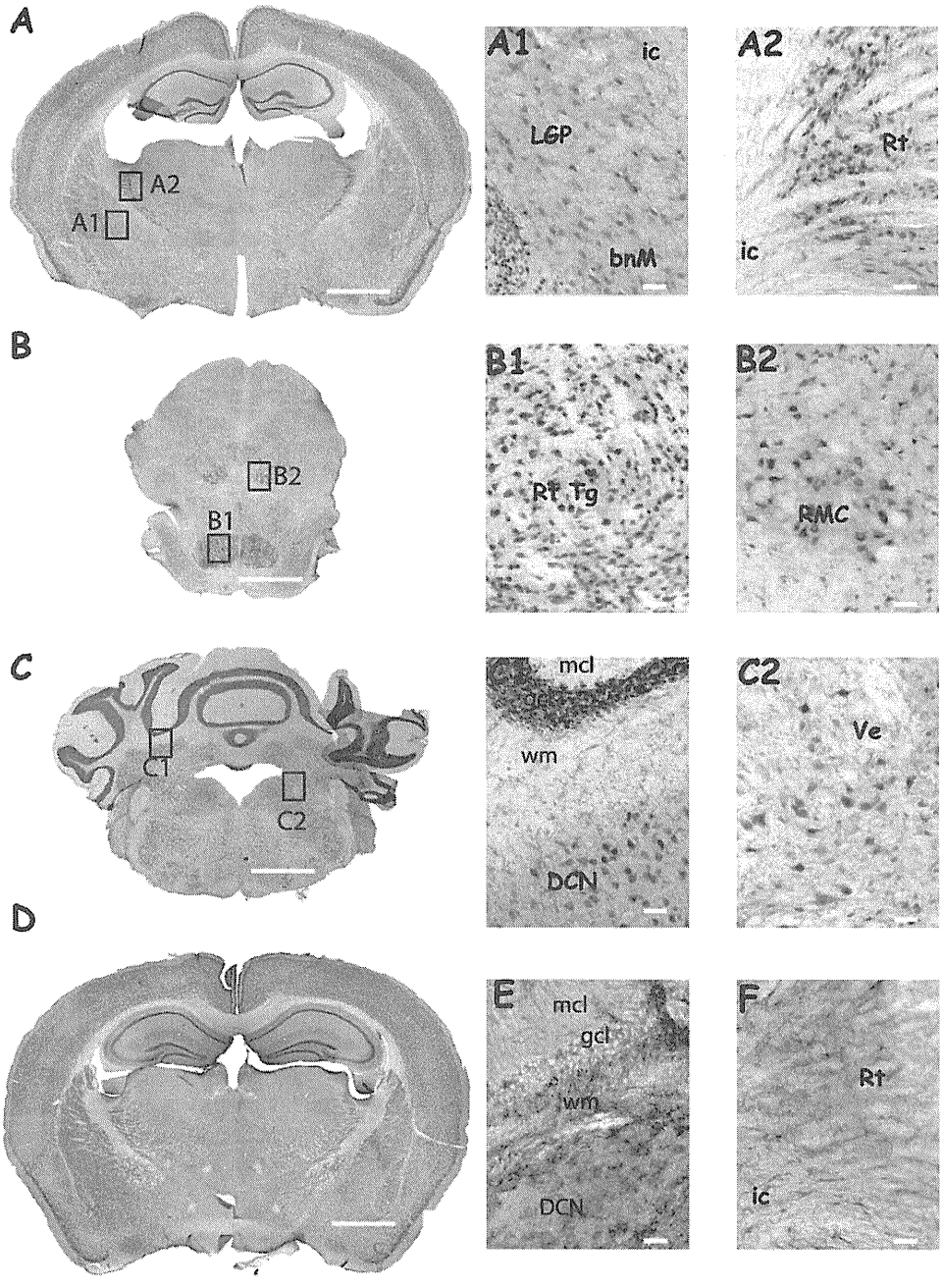

Fig. 1. X-gal staning in citrin-deficient mice. Coronal sections of citrin$^{-/-}$ (**A–C**) or citrin$^{+/+}$ (**D**) were stained for X-gal (blue) and counterstained for NeuN (brown). The areas indicated in A–C are shown at higher magnification in **A1–C2**. Note the absence of X-gal staining in D (compared with A) and also the regional colocalization of X-gal staining with NeuN-marked cells. The lack of regional colocalization with GFAP (as glial marker, brown) is shown in **E** (same region as in C1) and **F** (compare with A2). bnM, basal nuclei (Meynert); DCN, deep cerebellar nuclei; gcl, granule cell layer; ic, internal capsule; LGP, lateral globus pallidus; mcl, molecular cell layer; pcl, purkinje cell layer; Pn, pontine nuclei; RMC, red nuclei (magnocellular); Rt, reticular thalamic nuclei; Rt Tg, reticular tegmental nuclei of pons; tfp, transverse fibers of pons; Ve, vestibular nuclei. Scale bars = 1 mm in A–D; 50 μm in A1–C2,E,F.

tions were then mounted with mowiol for analysis in a confocal Zeiss microscope.

β-Galactosidase Activity Assays

Liver or brain extracts were taken from citrin$^{+/+}$ mice and from citrin$^{-/-}$ animals fed ad libitum, or 24 hr fasted, or 24 hr fasted plus 48 hr refed after sacrifice by cervical dislocation. Whole brains were divided in two at the level of the colliculus (midbrain). The anterior half containing the cortex, hippocampus, thalamus, and hypothalamus is hereafter termed *cortex*, and the posterior half containing the cerebellum and medulla is termed *cerebellum*. Both halves contained some midbrain. The cortex or cerebellum fractions were washed, minced, homogenized in IM [in mM: 250 sucrose, 25 Hepes, pH 7.4, 10 KCl, 1 EDTA, 1 EGTA, 1.5 $MgCl_2$, 1 dithiothreitol (DTT), 1 phenylmethylsulfonylfluoride (PMSF), 1 iodoacetamide], and centrifuged at 700*g*. The supernatant was further centrifuged at 10,000*g* to obtain the cytosolic fraction, in which the soluble β-gal is contained.

Enzyme activity was measured as described by Gow et al. (1992) and Miller (1972), with modifications. Briefly 50–100 μl (brain) or 10–20 μl (liver) cytosolic fractions were incubated in assay media [final concentration 60 mM

Na_2HPO_4, 40 mM NaH_2PO_4, 3.3 mM o-nitrophenol galactopyranoside (ONPG)]. Reactions in which the substrate ONPG was omitted from the assay media served as blanks. After color development (20 hr, liver; 40 hr, brain), $NaCO_3$ (0.5 M final) was added to terminate the reaction, and samples were centrifuged and read in a FLUOstar optima (BMG-Labtech) plate spectrophotometer at 410 nm. Activity values were expressed as DO/mg protein at the specified time point, after correction for the corresponding blank. No increase in absorbance was observed in samples from wild-type mice that lack β-galactosidase.

RESULTS

Citrin Localization in the Brain

The citrin (*SLC25A13*) knockout mice used in this study were obtained from Lexicon Pharmaceuticals, by gene-trapping as described earlier (Contreras et al., 2007), and the trapping vector contained lacZ. Therefore, in these lacZ knock-in mice, the expression of the β-galactosidase reporter is controlled by the endogenous regulatory elements of the *SLC25A13* gene, and the enzyme will be expressed at the same level and location as citrin in wild-type mice. The citrin expression pattern in the brain of young adult mice was identified by X-gal staining in brain sections of citrin$^{-/-}$ mice. This required very long incubation periods (72 hr of incubation with X-gal was needed), showing that citrin levels are extremely low. In addition, X-gal expression pattern was highly localized (Fig. 1, Table I). This explains why in previous studies we failed to detect citrin in the brain (Ramos et al., 2003).

The strongest expression was found in deep cerebellar nuclei and vestibular nuclei (Fig. 1C,C1,C2), reticular nuclei of the thalamus (Fig. 1A,A2), reticular tegmental nuclei of pons (Fig. 1B,B1), and red magnocellular nuclei (Fig. 1B,B2), although strong labelling was also obtained in septal nuclei, cochlear nuclei, and spinal trigeminal tract (Table I).

X-gal staining was observed mainly in cell bodies at restricted areas throughout the brain (Table I), although a punctate and/or diffuse pattern was sometimes observed at different locations. In those areas where cell bodies were clearly recognizable, there was a zonal colocalization with NeuN, in contrast to the situation observed with GFAP, with which no colocalization was detected (Fig. 1, compare A2 and F, C1 and E). Because colocalization at the cellular level was not clear in sections double stained for X-gal and NeuN or GFAP, samples were analyzed by confocal inmunofluorescence with antibodies against β-gal and NeuN or GFAP. The results shown in Figure 2 confirmed the lack of colocalization with the glial marker, insofar as the majority of the β-gal positive cells were also positive for NeuN (Fig. 2D–F, higher magnification G–I) and MAP2 (not shown). The lack of expression of LacZ in glial cells is not due to a difficulty of astrocytes with β-gal expression; the enzyme has been shown to colocalize with GFAP in other studies (de Leeuw et al., 2006; Lee et al., 2006; Karavanova et al., 2007). Thus, the results indicate that citrin is undetectable in glial cells and is expressed in neurons at very low levels.

TABLE I. Areas of Citrin Expression (X-Gal Deposits) in the Adult Mouse Brain

Zone	Expression level	Nuclei
Septum	+++, Cell bodies	Septal nuclei: vertical limb of diagonal band nu, medial septal nu, horiz diagonal band nu
Striatum/ hypothalamus	++, Cell bodies	Ventral pallidum
Hypothalamus	++, Cell bodies	Magnocellular preoptic nu
Striatum	+, Cell bodies	Caudate putamen: lateral globus pallidus, Meynert nu
Thalamus	++, Cell bodies	Reticular nucleus of thalamus; subthalamic nuc (zona incerta)
Midbrain	++++, Cell bodies	Magnocellular red nu
Pons	++++, Cell bodies	Pontine/reticular tegmental pontine nu
Cerebellum	++++, Cell bodies	Deep cerebellar nu
Medulla	+++, Cell bodies	Cochlear nu; spinal trigeminal tract, vestibular nu, lateral paragigantecellular nu
Tract regions	+, Punctate pattern	Cingulus; corpus callosum; stria terminalis; capsula externa/interna; anterior commisure; fimbria of hipocampus; globus pallidus; optic tract; fornix

Fasting Regulates Citrin Expression in the Brain

Citrin mRNA levels were found to be altered in some brain areas of mice during the fasting-to-refed transition (B. Thorens, unpublished observations). To verify whether there were similar changes in citrin expression in the whole brain, we have measured β-gal activity in mouse brain after a 24-hr fast and after refeeding. We have also measured β-gal activity in liver as control. As shown in Table II, there is an increase in β-gal activity (i.e., citrin expression) in mouse brain after a 24-hr fast, which returns to normal levels at 48 hr after normal eating. The effect is observed both in cortex and in cerebellum, and it is more prominent in the cerebellum. A similar but smaller fasting-related increase was observed in the liver (Table II).

DISCUSSION

Citrin is the hepatic isoform of the aspartate glutamate carrier and to date was thought to be absent from the nervous system, where aralar is the main isoform present (Begum et al., 2002; del Arco et al., 2002; Ramos et al., 2003). However, citrin was observed in cultured glial cells (Ramos et al., 2003), and citrin mRNA was also found by in situ hydridization in spinal

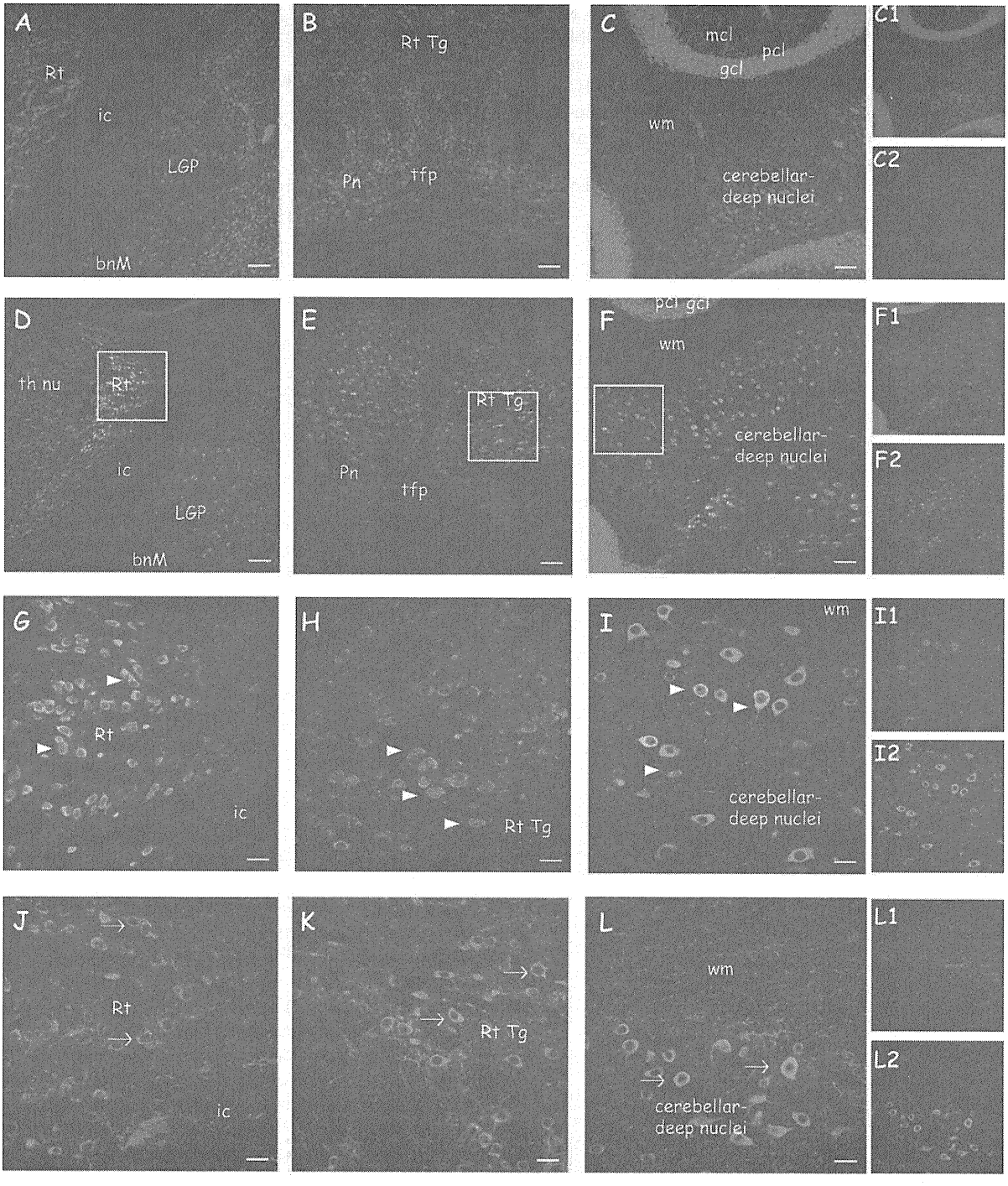

Fig. 2. Localization of β-gal expression in neurons. Brain sections of control (**A–C**) and citrin-deficient (**D–L**) mice were inmunostained with antibodies against β-gal (green) and either NeuN (neuronal marker, A–I, red) or GFAP (glial marker, J–L, red). Note colocalization of β-gal with discrete groups of cells marked with NeuN (D–I) and absence of colocalization with GFAP (J–L). **Insets** in D–F are shown at higher magnification in G–I. Similar regions are shown for GFAP (J–L). Right column shows the corresponding images of separated channels (1, NeuN or GFAP, red; and 2 β-gal, green) for C,F,I,L. B, basal nuceli (Meynert); gcl, granule cell layer; ic, internal capsule; LGP, lateral globus pallidus; mcl, molecular cell layer; pcl, purkinje cell layer; Pn, pontine nuclei; Rt, reticular thalamic nuclei; Rt Tg, reticular tegmental nuclei of pons; tfp, transverse fibers of pons. Scale bars = 100 μm in A–F; 25 μm in G–L.

TABLE II. β-Galactosidase Activity In Brain And Liver From Citrin$^{-/-}$ During a Fasting-to-Refed Transition†

	Control	24 Hours fasted (%)	48 Hours refed (%)
Cortex	1.99 ± 0.2	3.59 ± 0.6* (180)	2.43 ± 0.3 (122)
Cerebellum	4.72 ± 0.9	9.56 ± 1.5* (202)	6.1 ± 0.84 (129)
Liver	22.2 ± 1.9	37.3± 3.3** (168)	29.8 ± 4 (134)

†β-Galactosidase activity was measured as stated in Materials and Methods in cytosolic fractions of cortex, cerebellum (n = 5), and liver (n = 3) in citrin-deficient mice fed ad libitum (control), or 24-hr fasted, or 24-hr fasted plus 48-hr refed. Assays were performed in duplicate with blanks (no ONPG in medium). No β-galactosidase activity was detected in wild-type citrin mice. Results are expressed as DO/mg protein and are mean ± SE of five (brain) or three (liver) experiments performed in duplicate. Statistical difference (paired Student's *t*-test) with respect to control.
*$P < 0.05$.
**$P < 0.005$.

cord (www.brain-map.org). Here we present new evidence on the presence of the hepatic isoform of the AGC citrin, at very low levels, in the brain in a few restricted locations, particularly the deep cerebellar nuclei. Surprisingly, citrin expression is restricted to brain neurons, whereas astrocytes, which express citrin in culture (Ramos et al., 2003), do not express it in brain. The divergence between citrin expression in astrocytes in culture and in brain in vivo is consistent with the substantial differences in gene expression between FACS-isolated brain astrocytes and cultured astroglia (Cahoy et al., 2008). This is in contrast to cultures of other brain cells, such as oligodendrocytes or oligodendrocyte precursor cells, which have the same pattern of gene expression in culture and in vivo (Dugas et al., 2006), which indicates that cultured astroglia do not represent the same cell type as in vivo astrocyes but instead represent an astrocyte-like cell type (Cahoy et al., 2008). This may also explain why aralar, the main brain AGC, is readily detected in cultured astrocytes but not in brain astrocytes (Ramos et al., 2003).

A lack or very low levels of any of the AGCs in brain astrocytes imply an absence of a robust functional malate-aspartate shuttle and, therefore, a difficulty in transferring redox equivalents from the cytosol to the mitochondrial matrix. It is likely that brain astrocytes use the glycerol phosphate redox shuttle, whose presence in astrocytes has been demonstrated by the finding of enriched transcripts for the two members of the shuttle, cytosolic (GPD1) and mitochondrial (GPD2) glycerol-phosphate dehydrogenases (Lovatt et al., 2007; Cahoy et al., 2008), a colocalization that was not detected earlier (Leveille et al., 1980; Nguyen et al., 2003; McKenna et al., 2006). On the other hand, the results agree with the fact that glial metabolism is more glycolytic than that of neurons, and glial cells generate lactate to support the regeneration of NAD^+ in the cytosol (Winkler et al., 2000, 2004). Lactate would be then taken up and oxidized in neurons, which have a have a robust malate aspartate shuttle, as proposed by the astrocyte–neuron lactate shuttle hypothesis (Magistretti et al., 1999; Kasischke et al., 2004; Pellerin et al., 2007).

Lack of AGC isoforms in brain astroglia is also relevant to the metabolism of glutamate in glial mitochondria. In general, glutamate entry in mitochondria occurs through a glutamate-hydroxyl mitochondrial carrier (GC1/Slc25a22 or GC2/ Slc25a18) or the aspartate-glutamate exchangers aralar or citrin and is followed by formation of αKG via glutamate dehydrogenase or aspartate aminotransferase, respectively (Palmieri, 2004). However, inhibitor studies of glutamate metabolism on cultured astrocytes suggest that, whereas exogenous glutamate is oxidized via glutamate dehydrogenase and not via mitochondrial aspartate aminotransferase, glutamate arising endogenously from glutamine, a pathway that is not known to depend on the aspartate-glutamate mitochondrial carrier but possibly on mitochondrial glutamine carriers, is metabolized through mitochondrial aspartate aminotransferase (for reviews see McKenna et al., 2006; McKenna, 2007). These results agree with the presence of undetectable levels of AGCs on brain astroglial cells shown in this and previous studies. On the other hand, the fate of the aspartate produced in glial mitochondria, which has been shown to be readily labeled from 1-^{13}C-glucose in vivo (Navarro et al., 2008), demands further study.

We found that citrin expression is up-regulated in liver from fasted animals (Table II), as reported previously (Begum et al., 2002). This agrees with the elevation of malate dehydrogenase and aspartate transaminase (Sokolovic et al., 2008) and the increase in gluconeogenesis during fasting, which depend on MAS activity especially from reduced substrates (Strzelecki et al., 1988; Sugano et al., 1988; Satrustegui et al., 2007). Because there is no gluconeogenesis in brain, we hypothesized that citrin could be expressed at feeding and energy balance control centers of the brain, which sense glycemic changes. However, citrin expression was not found at any of the classical feeding control centers of the CNS [arcuate nucleus and other hypothalamic nuclei (Marty et al., 2007)]. Neurons in those centers sense changes in glucose and respond by changing their firing rate and secreting active neuropeptide that is orexigenic or anorexigenic (Oomura et al., 1964; Bady et al., 2006; Marty et al., 2007; Gao and Horvath, 2008). However, citrin is not enriched in any of these centers. Nonetheless, the cerebellar deep nuclei, where citrin is expressed most, appear to have a role in the regulation of nonsomatic activities, particularly visceral activities, associated with feeding behavior (Zhu and Wang, 2008). There are neural pathways that connect directly the deep cerebellar nuclei and hypothalamic nuclei involved in feeding control, and these cerebellohypothalamic projections form a bridge through which the cerebellum may participate in the regulation of food intake (Zhu et al., 2004; Zhu and Wang, 2008; Li et al., 2009). Determining whether citrin up-regulation is related to enhanced glucose or lactate utilization in specific neurons involved in feeding control or is merely a residual response to the same cues

as the liver, without any significant function in the brain, will require further clarification.

In the brain, aspartate is a precursor of N-acetylaspartate (NAA), the neuron-borne donor of acetyl groups in myelin lipid synthesis, and aralar deficiency causes a large drop of aspartate and NAA in the mouse brain, leading to hypomyelination (Jalil et al., 2005). The only aralar-deficient patient described so far presented a similar drop in NAA together with hypomyelination, arrested psychomotor development, hypotonia, and seizures (Wibom et al., 2009). However, in this patient, the defect in myelin synthesis seemed to be restricted to the cerebral cortices, insofar as white matter in cerebellum and brainstem appeared normal (Wibom et al., 2009). Although the expression levels of citrin in the mouse brain are very low, our results indicate that the deep cerebellar nuclei are the areas with higher citrin expression. This opens up the possibility that citrin might be expressed in the human cerebellum and might be able to rescue (at least partially) aspartate, NAA, and myelin synthesis in the cerebellum when aralar, the main AGC, is not functioning.

ACKNOWLEDGMENTS

We thank Barbara Sesé and Isabel Manso for excellent technical assistance. The CIBER de Enfermedades Raras is an initiative of the ISCIII.

REFERENCES

Bady I, Marty N, Dallaporta M, Emery M, Gyger J, Tarussio D, Foretz M, Thorens B. 2006. Evidence from glut2-null mice that glucose is a critical physiological regulator of feeding. Diabetes 55:988–995.

Begum L, Jalil MA, Kobayashi K, Iijima M, Li MX, Yasuda T, Horiuchi M, del Arco A, Satrustegui J, Saheki T. 2002. Expression of three mitochondrial solute carriers, citrin, aralar1 and ornithine transporter, in relation to urea cycle in mice. Biochim Biophys Acta 1574:283–292.

Berkich DA, Ola MS, Cole J, Sweatt AJ, Hutson SM, LaNoue KF. 2007. Mitochondrial transport proteins of the brain. J Neurosci Res 85:3367–3377.

Cahoy JD, Emery B, Kaushal A, Foo LC, Zamanian JL, Christopherson KS, Xing Y, Lubischer JL, Krieg PA, Krupenko SA, Thompson WJ, Barres BA. 2008. A transcriptome database for astrocytes, neurons, and oligodendrocytes: a new resource for understanding brain development and function. J Neurosci 28:264–278.

Contreras L, Gomez-Puertas P, Iijima M, Kobayashi K, Saheki T, Satrustegui J. 2007. Ca^{2+} Activation kinetics of the two aspartate-glutamate mitochondrial carriers, aralar and citrin: role in the heart malate-aspartate NADH shuttle. J Biol Chem 282:7098–7106.

Couegnas A, Schweitzer A, Andrieux A, Ghandour MS, Boehm N. 2007. Expression pattern of STOP lacZ reporter gene in adult and developing mouse brain. J Neurosci Res 85:1515–1527.

Dawson AG. 1979. Oxidation of cytosolic NADH formed during aerobic metabolism in mammalian cells. Trends Biochem Sci 4:171–176.

de Leeuw B, Su M, ter Horst M, Iwata S, Rodijk M, Hoeben RC, Messing A, Smitt PS, Brenner M. 2006. Increased glia-specific transgene expression with glial fibrillary acidic protein promoters containing multiple enhancer elements. J Neurosci Res 83:744–753.

del Arco A, Satrustegui J. 1998. Molecular cloning of aralar, a new member of the mitochondrial carrier superfamily that binds calcium and is present in human muscle and brain. J Biol Chem 273:23327–23334.

del Arco A, Agudo M, Satrustegui J. 2000. Characterization of a second member of the subfamily of calcium-binding mitochondrial carriers expressed in human non-excitable tissues. Biochem J 345:725–732.

del Arco A, Morcillo J, Martinez-Morales JR, Galian C, Martos V, Bovolenta P, Satrustegui J. 2002. Expression of the aspartate/glutamate mitochondrial carriers aralar1 and citrin during development and in adult rat tissues. Eur J Biochem 269:3313–3320.

Dugas JC, Tai YC, Speed TP, Ngai J, Barres BA. 2006. Functional genomic analysis of oligodendrocyte differentiation. J Neurosci 26:10967–10983.

Gao Q, Horvath TL. 2008. Neuronal control of energy homeostasis. FEBS Lett 582:132–141.

Gellerich FN, Gizatullina Z, Nguyen HP, Trumbeckaite S, Vielhaber S, Seppet E, Zierz S, Landwehrmeyer B, Riess O, von Horsten S, Striggow F. 2008. Impaired regulation of brain mitochondria by extramitochondrial Ca^{2+} in transgenic Huntington disease rats. J Biol Chem 283:30715–30724.

Gow A, Friedrich VL, Jr., Lazzarini RA. 1992. Myelin basic protein gene contains separate enhancers for oligodendrocyte and Schwann cell expression. J Cell Biol 119:605–616.

Indiveri C, Dierks T, Kramer R, Palmieri F. 1991. Reaction mechanism of the reconstituted oxoglutarate carrier from bovine heart mitochondria. Eur J Biochem 198:339–347.

Jalil MA, Begum L, Contreras L, Pardo B, Iijima M, Li MX, Ramos M, Marmol P, Horiuchi M, Shimotsu K, Nakagawa S, Okubo A, Sameshima M, Isashiki Y, Del Arco A, Kobayashi K, Satrustegui J, Saheki T. 2005. Reduced N-acetylaspartate levels in mice lacking aralar, a brain- and muscle-type mitochondrial aspartate-glutamate carrier. J Biol Chem 280:31333–31339.

Karavanova I, Vasudevan K, Cheng J, Buonanno A. 2007. Novel regional and developmental NMDA receptor expression patterns uncovered in NR2C subunit-beta-galactosidase knock-in mice. Mol Cell Neurosci 34:468–480.

Kasischke KA, Vishwasrao HD, Fisher PJ, Zipfel WR, Webb WW. 2004. Neural activity triggers neuronal oxidative metabolism followed by astrocytic glycolysis. Science 305:99–103.

Kobayashi K, Sinasac DS, Iijima M, Boright AP, Begum L, Lee JR, Yasuda T, Ikeda S, Hirano R, Terazono H, Crackower MA, Kondo I, Tsui LC, Scherer SW, Saheki T. 1999. The gene mutated in adult-onset type II citrullinaemia encodes a putative mitochondrial carrier protein. Nat Genet 22:159–163.

Lee Y, Su M, Messing A, Brenner M. 2006. Astrocyte heterogeneity revealed by expression of a GFAP-LacZ transgene. Glia 53:677–687.

Leveille PJ, McGinnis JF, Maxwell DS, de Vellis J. 1980. Immunocytochemical localization of glycerol-3-phosphate dehydrogenase in rat oligodendrocytes. Brain Res 196:287–305.

Li B, Guo CL, Tang J, Zhu JN, Wang JJ. 2009. Cerebellar fastigial nuclear inputs and peripheral feeding signals converge on neurons in the dorsomedial hypothalamic nucleus. Neurosignals 17:132–143.

Lovatt D, Sonnewald U, Waagepetersen HS, Schousboe A, He W, Lin JH, Han X, Takano T, Wang S, Sim FJ, Goldman SA, Nedergaard M. 2007. The transcriptome and metabolic gene signature of protoplasmic astrocytes in the adult murine cortex. J Neurosci 27:12255–12266.

Magistretti PJ, Pellerin L, Rothman DL, Shulman RG. 1999. Energy on demand. Science 283:496–497.

Marmol P, Pardo B, Wiederkehr A, del Arco A, Wollheim CB, Satrustegui J. 2009. Requirement for aralar and its Ca^{2+}-binding sites in Ca^{2+} signal transduction in mitochondria from INS-1 clonal beta-cells. J Biol Chem 284:515–524.

Marty N, Dallaporta M, Thorens B. 2007. Brain glucose sensing, counterregulation, and energy homeostasis. Physiology 22:241–251.

McKenna MC. 2007. The glutamate-glutamine cycle is not stoichiometroc: fates of glutamate in the brain. J Neurosci Res 85:3347–3358.

McKenna MC, Waagepetersen HS, Schousboe A, Sonnewald U. 2006. Neuronal and astrocytic shuttle mechanisms for cytosolic-mitochondrial transfer of reducing equivalents: current evidence and pharmacological tools. Biochem Pharmacol 71:399–407.

Miller JH. 1972. Experiments in molecular genetics. Cold Spring Harbor, NY: Cold Spring Harbor Laboratory.

Navarro D, Zwingmann C, Butterworth RF. 2008. Region-selective alterations in glucose oxidation and amino acid synthesis in the thiamine-deficient rat brain: a re-evaluaction using $^{1}H/^{13}C$ nuclear magnetic resonance spectroscopy. J Neurochem 106:603–612.

Nguyen NH, Brathe A, Hassel B. 2003. Neuronal uptake and metabolism of glycerol and the neuronal expression of mitochondrial glycerol-3-phosphate dehydrogenase. J Neurochem 85:831–842.

Oomura Y, Kimura K, Ooyama H, Maeno T, Iki M, Kuniyoshi M. 1964. Reciprocal activities of the ventromedial and lateral hypothalamic areas of cats. Science 143:484–485.

Palmieri F. 2004. The mitochondrial transporter family (SLC25): physiological and pathological implications. Pflugers Arch Eur J Physiol 447:689–709.

Palmieri L, Pardo B, Lasorsa FM, del Arco A, Kobayashi K, Iijima M, Runswick MJ, Walker JE, Saheki T, Satrustegui J, Palmieri F. 2001. Citrin and aralar1 are Ca^{2+}-stimulated aspartate/glutamate transporters in mitochondria. EMBO J 20:5060–5069.

Pardo B, Contreras L, Serrano A, Ramos M, Kobayashi K, Iijima M, Saheki T, Satrustegui J. 2006. Essential role of aralar in the transduction of small Ca^{+} signals to neuronal mitochondria. J Biol Chem 281:1039–1047.

Pellerin L, Bouzier-Sore AK, Aubert A, Serres S, Merle M, Costalat R, Magistretti PJ. 2007. Activity-dependent regulation of energy metabolism by astrocytes: an update. Glia 55:1251–1262.

Ramos M, del Arco A, Pardo B, Martinez-Serrano A, Martinez-Morales JR, Kobayashi K, Yasuda T, Bogonez E, Bovolenta P, Saheki T, Satrustegui J. 2003. Developmental changes in the Ca^{2+}-regulated mitochondrial aspartate-glutamate carrier aralar1 in brain and prominent expression in the spinal cord. Brain Res Dev Brain Res 143:33–46.

Satrustegui J, Pardo B, Del Arco A. 2007. Mitochondrial transporters as novel targets for intracellular calcium signaling. Physiol Rev 87:29–67.

Smith VR, Walker JE. 2003. Purification and folding of recombinant bovine oxoglutarate/malate carrier by immobilized metal-ion affinity chromatography. Protein Expr Purif 29:209–216.

Sokolovic M, Sokolovic A, Wehkamp D, Ver Loren van Themaat E, de Waart DR, Gilhuijs-Pederson LA, Nikolsky Y, van Kampen AH, Hakvoort TB, Lamers WH. 2008. The transcriptomic signature of fasting murine liver. BMC Genom 9:528.

Strzelecki T, Strzelecka D, Koch CD, LaNoue KF. 1988. Sites of action of glucagon and other Ca^{2+} mobilizing hormones on the malate aspartate cycle. Arch Biochem Biophys 264:310–320.

Sugano T, Nishimura K, Sogabe N, Shiota M, Oyama N, Noda S, Ohta M. 1988. Ca^{2+}-dependent activation of the malate-aspartate shuttle by norepinephrine and vasopressin in perfused rat liver. Arch Biochem Biophys 264:144–154.

Walker JE, Runswick MJ. 1993. The mitochondrial transport protein superfamily. J Bioenerg Biomembr 25:435–446.

Watkins J, Basu S, Bogenhagen DF. 2008. A quantitative proteomic analysis of mitochondrial participation in p19 cell neuronal differentiation. J Proteome Res 7:328–338.

Wibom R, Lasorsa FM, Töhönen V, Barbaro M, Sterky FH, Kucinski M, Naess N, Jonsson M., Pierri CL, Palmieri F, Wedell A. 2009. AGC1 deficiency associated with global cerebral hypomyelination. N Engl J Med 361:489–495.

Winkler BS, Arnold MJ, Brassell MA, Puro DG. 2000. Energy metabolism in human retinal Muller cells. Invest Ophthalmol Vis Sci 41:3183–3190.

Winkler BS, Starnes CA, Sauer MW, Firouzgan Z, Chen SC. 2004. Cultured retinal neuronal cells and Muller cells both show net production of lactate. Neurochem Int 45:311–320.

Xu Y, Ola MS, Berkich DA, Gardner TW, Barber AJ, Palmieri F, Hutson SM, LaNoue KF. 2007. Energy sources for glutamate neurotransmission in the retina: absence of the aspartate/glutamate carrier produces reliance on glycolysis in glia. J Neurochem 101:120–131.

Zhu JN, Wang JJ. 2008. The cerebellum in feeding control: possible function and mechanism. Cell Mol Neurobiol 28:469–478.

Zhu JN, Zhang YP, Song YN, Wang JJ. 2004. Cerebellar interpositus nuclear and gastric vagal afferent inputs reach and converge onto glycemia-sensitive neurons of the ventromedial hypothalamic nucleus in rats. Neurosci Res 48:405–417.

Journal of Cerebral Blood Flow & Metabolism (2011) 31, 90–101

www.jcbfm.com

Brain glutamine synthesis requires neuronal-born aspartate as amino donor for glial glutamate formation

Beatriz Pardo[1], Tiago B Rodrigues[2,3], Laura Contreras[1,7], Miguel Garzón[4], Irene Llorente-Folch[1], Keiko Kobayashi[5], Takeyori Saheki[6], Sebastian Cerdan[2] and Jorgina Satrústegui[1]

[1]*Departamento de Biología Molecular, Centro de Biología Molecular Severo Ochoa UAM-CSIC, and CIBER de Enfermedades Raras (CIBERER), Universidad Autónoma de Madrid, Madrid, Spain;* [2]*Instituto de Investigaciones Biomédicas 'Alberto Sols' CSIC-UAM, Madrid, Spain;* [3]*Centro de Neurociências e Biologia Celular e Departamento de Bioquímica, Faculdade de Ciências e Tecnologia, Universidade de Coimbra, Coimbra, Portugal;* [4]*Department of Anatomy, Histology and Neuroscience, School of Medicine, Universidad Autónoma de Madrid, Madrid, Spain;* [5]*Department of Molecular Metabolism and Biochemical Genetics, Kagoshima University Graduate School of Medical and Dental Sciences, Kagoshima, Japan;* [6]*Institute for Health Sciences, Tokushima Bunri University, Yamashiro-cho, Tokushima, Japan*

The glutamate–glutamine cycle faces a drain of glutamate by oxidation, which is balanced by the anaplerotic synthesis of glutamate and glutamine in astrocytes. *De novo* synthesis of glutamate by astrocytes requires an amino group whose origin is unknown. The deficiency in *Aralar*/*AGC1*, the main mitochondrial carrier for aspartate–glutamate expressed in brain, results in a drastic fall in brain glutamine production but a modest decrease in brain glutamate levels, which is not due to decreases in neuronal or synaptosomal glutamate content. *In vivo* ^{13}C nuclear magnetic resonance labeling with $^{13}C_2$acetate or (1-^{13}C) glucose showed that the drop in brain glutamine is due to a failure in glial glutamate synthesis. *Aralar* deficiency induces a decrease in aspartate content, an increase in lactate production, and lactate-to-pyruvate ratio in cultured neurons but not in cultured astrocytes, indicating that Aralar is only functional in neurons. We find that aspartate, but not other amino acids, increases glutamate synthesis in both control and aralar-deficient astrocytes, mainly by serving as amino donor. These findings suggest the existence of a neuron-to-astrocyte aspartate transcellular pathway required for astrocyte glutamate synthesis and subsequent glutamine formation. This pathway may provide a mechanism to transfer neuronal-born redox equivalents to mitochondria in astrocytes.
Journal of Cerebral Blood Flow & Metabolism (2011) **31,** 90–101; doi:10.1038/jcbfm.2010.146; published online 25 August 2010

Keywords: AGC1; Aralar; aspartate; glial glutamine; mitochondrial aspartate–glutamate carrier; OmniBank

Introduction

Glutamate is the main excitatory neurotransmitter in the central nervous system. The lack of pyruvate carboxylase in neurons makes them incapable of *de novo* synthesis of glutamate and γ-aminobutyric acid (GABA) from glucose (Shank *et al*, 1985). However, the release of glutamate is followed by uptake into astrocytes rather than neurons (Schousboe, 1981). This leads to a continuous drain of glutamate from neurons to astrocytes, which needs to be compensated through the supply of a glutamate precursor formed in astrocytes, glutamine. The glutamate–glutamine cycle for glutamatergic neurons and the GABA–glutamine cycle for GABAergic ones account for glutamate homeostasis in the corresponding terminals (Bak *et al*, 2006). In addition to transcellular cycling, some of the glutamate–glutamine is oxidized in the brain, about 10% to 30% under basal conditions (Rothman *et al*, 2003; Hertz and Kala, 2007) leading to a net loss of these compounds from the glutamate–glutamine cycle

Correspondence: Professor J Satrústegui, Departamento de Biología Molecular, Centro de Biología Molecular 'Severo Ochoa' UAM-CSIC, c/Nicolás Cabrera 1, Universidad Autónoma de Madrid, Cantoblanco, Madrid 28049, Spain.
E-mail: jsatrustegui@cbm.uam.es
[7]Current address: Department of Biomedical Sciences, University of Padua, Viale Giuseppe Colombo, 3-35121 Padua, Italy.
This work was supported in part by Ministerio de Educación y Ciencia Grants BFU2008-04084/BMC (to JS) and SAF2008-01327 (to SC), Comunidad de Madrid Grants S-GEN-0269-2006 MITOLAB-CM (to JS) and S-BIO-2006-0170 MULTIMAG (to SC), European Union Grant LSHM-CT-2006-518153 (to JS), and Fundación Médica Mutua Madrileña (to BP). The CIBER de Enfermedades Raras is an initiative of the ISCIII.
Received 21 April 2010; revised 25 July 2010; accepted 27 July 2010; published online 25 August 2010

(McKenna, 2007; Schousboe *et al*, 1993; Sonnewald *et al*, 1993; Gamberino *et al*, 2007). This requires a continuous replenishment of glutamate and glutamine in astrocytes. Therefore, the small glial pool of glutamate, which is the precursor of the glutamine pool, is rapidly turning over (Cruz and Cerdán, 1999).

De novo glutamate and glutamine production in astrocytes requires the supply of one or two ammonia groups, respectively, and neurons are thought to supply one or both (reviewed in Bak *et al* (2006)). Two mechanisms have been proposed for the effective transfer of ammonia for amidation in the glutamine synthesis reaction: (1) ammonia (NH_3) or ammonium (NH_4^+) transport (Bak *et al*, 2006) and (2) alanine-lactate nitrogen shuttle (Bak *et al*, 2006). The branched chain amino acid (BCAA)-branched chain keto acid nitrogen shuttle has been proposed to account for nitrogen donation to the glutamate amino group for net synthesis of glutamine involving pyruvate carboxylation (Lieth *et al*, 2001). The extent to which each of these processes actually supports glutamate and/or glutamine production in brain astrocytes, has not been established yet.

We now present evidence suggesting that aspartate is the neuron-born nitrogen donor for glial glutamate synthesis. The evidence was obtained in mice deficient in Aralar, the mitochondrial transporter of aspartate–glutamate present mainly in neurons (Ramos *et al*, 2003; Berkich *et al*, 2007; Xu *et al*, 2007). *Aralar*-KO mice have hypomyelination and a very drastic fall in brain aspartate and *N*-acetylaspartate (NAA) levels, because of lack of the only mitochondrial carrier that transports aspartate from the mitochondrial matrix to the cytosol in exchange for glutamate (Jalil *et al*, 2005). Similar features are present in a patient with Aralar deficiency (Wibom *et al*, 2009). We find that these mice have a marked decrease in the brain glutamine pool, but a more moderate decrease in the glutamate pool, consistent with a failure to produce glutamate and glutamine in the glial compartment. *In vivo* ^{13}C-labeling experiments with (^{13}C) acetate or glucose showed a dramatic loss of ^{13}C-labeled glutamine in *Aralar*-KO mice, indicating a decrease in glutamine synthesis. Cultured astrocytes, from both wild-type (WT) and *Aralar*-KO mice, were able to use aspartate to produce glutamate and glutamine from glucose at concentrations in which GABA, alanine, or leucine were essentially ineffective, showing that brain aspartate, which is produced mainly in neurons is probably used as preferred nitrogen donor for glutamate and glutamine synthesis in astrocytes.

Materials and methods

Animals and Genotypes

Male SVJ129 × C57BL6 mice carrying a deficiency for ARALAR expression (*Aralar*$^{-/-}$, *Aralar*$^{+/-}$, and *Aralar*$^{+/+}$) were obtained from Lexicon Pharmaceuticals, Inc (The Woodlands, TX, USA) (Jalil *et al*, 2005). The mice were housed in a humidity- and temperature-controlled room on a 12-hour light/dark cycle, receiving water and food *ad libitum*. Genotype was determined by PCR using genomic DNA obtained from tail or embryonic tissue samples (Nucleospin tissue kit, Macherey-Nagel, Dueren, Germany) as described previously (Jalil *et al*, 2005). All the experimental protocols used in this study were approved by the local Ethics Committees at the Center of Molecular Biology 'Severo Ochoa,' Autonoma University (UAM), Madrid, and at the Institute of Biomedical Research 'Alberto Sols' CSIC-UAM, Madrid, Spain.

Immunofluorescence

Animals were anesthetized by chloral hydrate (0.5 mg/g body weight; Sigma-Aldrich, St Louis, MO, USA) and perfused transcardially with saline buffer (0.9% NaCl in phosphate buffer) and then with 4% formaldehyde in phosphate buffer (formalin fixative). Brains were carefully removed and postfixed overnight in formalin (4°C) and transferred into sucrose (30% in phosphate buffer). Later, they were embedded in OCT compound (Tissue-Tek, Sakura Finetek Europe BV, Zoeterwoude, The Netherlands), frozen on dry ice and cut into 12 series of 30 μm coronal sections with a cryotome (free-floating sections). Sections were kept in cryoprotectant medium (25% glycerol, 25% ethylene glycol in 50 mmol/L phosphate buffer) and stored at −20°C until processing.

For immunofluorescence assay, cryoprotectant medium was washed with phosphate-buffered saline (PBS) before incubation in antigen retrieval medium (0.1% sodium dodecyl sulfate, 2 mmol/L EGTA (ethylene glycol-bis (2-amino-ethylether)-N,N,N′,N′-tetra-acetic acid), PBS) for 30 minutes at 37°C. Then sections were washed (PBS) and treated with $NaBH_4$ (5 mg/mL) to quench endogenous autofluorescence. Afterwards, sections were preincubated in PBS with 10% horse serum and 0.5% Triton X-100, and then incubated overnight with anti-Aralar (1:100, polyclonal) and anti-Cox-I (1:100, Molecular Probes, Eugene, OR, USA; monoclonal) in PBS with 2% horse serum and 0.25% Triton X-100. Secondary antibodies Alexa 488 (Molecular Probes, 1:500) and Cy3 mAB (Jackson Inmunoresearch Laboratories Inc., West Grove, PA, USA, 1:500) were incubated for 1 to 2 hours before mounting with mowiol. TOPRO-3 ({1-(4-[3-methyl-2,3-dihydro-(benzo-1,3-thiazole)-2-propylidene]-quinolinium)-3-trimethylammonium propane diodide} (TP3)) (Invitrogen, Carlsbad, CA, USA; 1:750) was used as nuclear probe. Imaging was performed in a confocal Zeiss microscope.

Electron Microscopy

Electron microscopy of brain sections from wt and Aralar-KO mice, immunocytochemical detection of Aralar, and identification of profiles for different cell types is described in Supplementary Materials and methods.

Amino-Acid Analysis in Brain Tissue and Astroglial and Neuronal Cells

For analysis in brain, mice were anesthetized, and cerebral metabolism was arrested using high-power (5 kW) microwaves (Muramatsu, Osaka, Japan). The whole brain was immediately removed from the skull on dry ice and homogenized with four volumes of 3% sulfosalicylic or 5% perchloric acid as described earlier (Jalil *et al*, 2005). The sulfosalicylic acid supernatants were used for amino-acid analysis with a JEOL JLC-500 amino-acid analyzer (JEOL Ltd., Tokyo, Japan); and the neutralized perchloric acid extracts were quantified with a Biochrom 20 amino-acid analyzer (Pharmacia, Uppsala, Sweden) as described below.

For analysis in cell cultures, both media and cells were processed in 3% perchloric acid neutralized and centrifuged at 10,000*g* for 15 minutes. Samples were lyophilized and dissolved in lithium citrate loading buffer 0.2 mol/L pH 2.2 for quantification with an automatic amino-acid analyzer Biochrom 20 using a precolumn derivatization with ninhydrin and a cationic exchange column. Glutamine and glutamate content was also measured in astroglial cultures by end point enzymatic reactions as described in Supplementary Materials and methods.

Glutamate content in cerebellar neurons was also assayed in Triton-permeabilized cells grown on glass coverslips by online fluorimetry as described in Supplementary Materials and methods for synaptosomes.

Glucose, Lactate, and Pyruvate Determinations in Media from Glial and Neuronal Cell Cultures

The concentrations of glucose, lactate, and pyruvate in culture media were quantified by using enzymatic kits from Boehringer (Phoenix, AZ, USA), BioVision (Mountain View, CA, USA), and INstruchemie BV (Delfzijl, The Netherlands), respectively, following in each case the manufacturer's instructions. All essays were performed in 48-well microplates, with a FLUOstar OPTIMA reader in the absorbance mode.

In Vivo ^{13}C-Labeling Studies

The experiments were conducted at postnatal Day 20. Animals from each group (16 WT and 16 *Aralar*-KO mice) were weighed and deeply anesthetized with an intraperitoneal injection of a mixture of Ketolar (ketamine; 40 μg/g body weight) and Domtor (medetomidine; 1 μg/g body weight) just before the ^{13}C substrate administration. Anesthesia was used in these experiments, as most of the mice were subjected to *in vivo* ^{1}H nuclear magnetic resonance spectroscopy analysis (results not shown) before metabolic-labeling experiments. Some of these mice (10 WT and 9 *Aralar*-KO) were intraperitoneally injected with (1-^{13}C) glucose (2 mmol/100 g body weight) and six animals of each genotype were intraperitoneally injected with (1,2-$^{13}C_2$) acetate (6 mmol/100 g body weight). Under these labeling conditions, the calculated initial plasma acetate concentration is several fold higher than the *Km* for its glial transporter (9 mmol/L; Waniewski and Martin, 1998). At this acetate concentration, neurons will also take up acetate by diffusion and metabolize it through acetate thiokinase, as the preference of astrocytes for acetate is due to transport (Waniewski and Martin, 1998). The physiological state of the animal was followed through all the experiment. Respiratory rate was monitored by a Biotrig system (Bruker Medical GmbH, Ettlingen, Germany), and body temperature was maintained at ~37°C using a thermostatic blanket and a temperature-regulated circulating water bath. Fifteen minutes after ^{13}C-label administration, the metabolism was arrested using a high-power (5 kW) focused microwave fixation system (Muromachi Kikai Co. Ltd., Tokyo, Japan). The brain was rapidly removed from the skull and immediately frozen in liquid N_2. (1-^{13}C) glucose (99.9% ^{13}C) and (1,2-$^{13}C_2$) acetate were obtained from Cambridge Isotope Laboratories (Andover, MA, USA). $^{2}H_2O$ (99.9% ^{2}H) was acquired from Apollo Scientific Ltd. (Stockport, Cheshire, CT, USA). The preparation of perchloric acid extracts of the individual biopsies (whole brain including cerebellum) and the procedures to carry out ^{13}C nuclear magnetic resonance spectroscopy are described in Supplementary Materials and methods.

Statistical Analysis

Statistical analysis was performed using the SPSS package (SAS Institute Inc., Cary, NC, USA). The statistical significance of the differences was assessed by one-way analysis of variance followed by a *post hoc* Student's, Duncan/Tukey, or Student–Newman–Keuls *t*-test method, as indicated. The results are expressed as mean ± standard error of the mean (s.e.m.).

Results

Brain Astrocytes have Limited Aralar/AGC1 Levels and Malate-Aspartate Shuttle Activity

We and others (Ramos *et al*, 2003; Berkich *et al*, 2007; Xu *et al*, 2007; Cahoy *et al*, 2008) have reported a preferential localization of Aralar mRNA and protein in neuron-rich areas in the postnatal mouse brain. In culture, neurons have much higher levels of Aralar protein than cultured glial cells (Ramos *et al*, 2003). Moreover, cultured astroglial cells express not only Aralar protein but also Citrin/AGC2 (Ramos *et al*, 2003; Supplementary Figure 1), an AGC isoform expressed in liver but hardly at all in brain, where it is expressed at very low levels only in a few neuronal clusters (Contreras *et al*, 2010), questioning the relevance of cultured astrocytes as reporters of brain astroglial cells. The brain from *Aralar*-KO mice has very low aspartate and NAA levels (Jalil *et al*, 2005), and because these two molecules are produced mainly by neurons and oligodendrocyte precursors (Urenjak *et al*, 1993), their fall in the brain from *Aralar*-KO mice was attributed to the lack of neuronal Aralar (Jalil *et al*, 2005). However, recent data from Lovatt *et al* (2007) suggested that Aralar mRNA is equally represented in brain astroglial cells and

neurons, and it was concluded that malate-aspartate shuttle had low and similar levels in both cell types.

To clarify the role of Aralar in aspartate formation and the malate-aspartate shuttle activity in the two cell types, we have first studied cell aspartate levels and redox shuttle activity in astrocytes and neuronal cultures derived from wild-type and *Aralar*-KO mice. Cultured astrocytes from *Aralar*$^{(+/+)}$, *Aralar*$^{(+/-)}$, and *Aralar*$^{(-/-)}$ mice show a dose-dependent loss of Aralar, whereas citrin levels were unchanged (Supplementary Figure 1). However, the lack of Aralar resulted in a prominent decrease in aspartate levels in neurons, but not in astrocytes (Table 1). Aralar deficiency increased by almost twofold lactate production in neurons resulting in a rise in the lactate-to-pyruvate ratio (by about 13-fold); however, lactate production and the lactate-to-pyruvate ratio were not significantly increased in the culture medium of astrocytes (Table 2), even though astrocytes have much higher capacity to stimulate glycolysis than neurons (Herrero-Mendez *et al*, 2009). These results show that Aralar in astroglial cells is not significantly required for aspartate production and that these cells do not rely on the malate-aspartate shuttle to transfer redox equivalents to mitochondria. As the glucose concentration used in these studies was higher than physiological (25 to 30 mmol/L), glucose utilization and lactate production have also been measured at 5 mmol/L glucose in short-term experiments (2 hours). Aralar deficiency resulted in the same increase in lactate production in neuronal but not astrocyte cultures (results not shown).

Taken together, the results show that neurons depend on Aralar for aspartate production, malate-aspartate shuttle activity and glucose oxidation, and cultured astrocytes, even though expressing Aralar, do not.

We have next studied the distribution of Aralar in the brain with the use of Aralar immunofluorescence. Colabeling with cytochrome oxidase antibodies was clearly observed in well-characterized neuronal regions (Figures 1A–1C), but not in the brain of *Aralar*-KO mice (Supplementary Figure 2). To further clarify the lack of Aralar in glial mitochondria, electron microscopy analysis in vibratome sections was performed (Figures 1D–1F). A very high proportion of Aralar-immunogold labeling was localized to neurons (94.1% ± 18.0%) in comparison to glial profiles (7.2% ± 0.5%; $P=0.0001$). In neurons (Figures 1D–1F), Aralar showed a prominent localization in mitochondria

Table 1 Cellular content of amino acids (nmol/mg protein) in extracts of cortical astroglial and cortical neuronal cultures from wild-type and *Aralar*-KO mice

	Astrocytes		*Neurons*	
	Wild type	*Aralar-KO*	*Wild type*	*Aralar-KO*
Phosphoserine	62.6 ± 4.7	78.9 ± 3.9	37.3 ± 0.3	50.8 ± 13.8
Aspartate	8.7 ± 1.2	7.9 ± 1.0	25.4 ± 1.3	6.2 ± 0.8***
Threonine	35.8 ± 3.7	48.9 ± 0.8	52.8 ± 5.9	74.4 ± 23.1
Serine	54.0 ± 5.6	75.1 ± 9.1	95.8 ± 6.9	111.6 ± 24.4
Glutamate	126.9 ± 14.5	160.8 ± 17.3	105.8 ± 11.1	120.8 ± 28.5
Glutamine	213.5 ± 15.2	289.6 ± 8.0*	39.0 ± 5.2	41.8 ± 10.1
Glycine	64.1 ± 9.4	108.8 ± 33.7	160.6 ± 19.3	309.5 ± 97.3
Alanine	12.1 ± 1.0	15.9 ± 1.8	9.8 ± 1.2	4.6 ± 0.8*
Valine	18.0 ± 1.4	29.6 ± 1.1	24.5 ± 2.8	30.4 ± 4.6
Isoleucine	16.2 ± 0.8	25.3 ± 1.3**	21.7 ± 2.5	25.7 ± 3.0
Leucine	15.8 ± 0.6	25.3 ± 1.4**	20.3 ± 2.3	22.8 ± 2.6
Lysine	19.9 ± 1.2	29.9 ± 3.4*	35.9 ± 3.4	64.5 ± 14.9
GABA	ND	ND	13.1 ± 0.7	17.3 ± 2.6

DMEM, Dulbecco's modified Eagle medium; GABA, γ-aminobutyric acid; ND, not detectable.
Cortical astrocytes and neurons in culture were maintained in DMEM media containing 25 mmol/L glucose supplemented with 10% serum or NB-B27 containing 30 mmol/L glucose, respectively. All media were aspartate free and contained 0.5 mmol/L (neurons) or 4.5 mmol/L (astrocytes) glutamine. Media was renewed 24 hours before recollecting cellular extracts at 14 (for astrocytes) or 10 DIV (for neurons). Amino acids were quantified with an automatic amino-acid analyzer Biochrom 20 using a cationic exchange column and precolumn derivatization with ninhydrin. Results are presented as mean ± s.e.m. ($n=4$). Data were statistically evaluated by one-way analysis of variance followed by Student's *t*-test. Comparisons between control and *Aralar*-deficient cultures were significant where indicated ***$P\leqslant0.001$; **$P\leqslant0.01$; *$P\leqslant0.05$.

Table 2 Glucose and pyruvate consumption, and lactate net formation measured in culture media of astroglial and neuronal cultures from wild-type (WT) and *Aralar*-KO (KO) mice

Cell type	*Genotype*	*Glucose consumed (μmol/mg prot/24 h)*	*Lactate net formation (μmol/mg prot/24 h)*	*Pyruvate consumed (μmol/mg prot/24 h)*	*Lact/Pyr ratio*
Astrocytes	WT	278.1 ± 2.7	152.14 ± 18.8	5.8 ± 0.1	348.7 ± 30.5
	KO	295.1 ± 22.2	176.3 ± 4.4	5.8 ± 0.0	446.6 ± 27.5
Neurons	WT	259.0 ± 3.5	10.3 ± 0.9	3.6 ± 0.0	49.8 ± 3.0
	KO	174.0 ± 9.8***	18.5 ± 0.7***	3.8 ± 0.0***	638.7 ± 196.6*

DMEM, Dulbecco's modified Eagle medium; Ext Gluc, extracellular glucose; GABA, γ-aminobutyric acid; Lac, Lactate; Pyr, Pyruvate.
Cortical astrocytes and neurons were cultured for 14 and 10 DIV, respectively, and subsequently incubated for 24 hours in DMEM containing 25 mmol/L glucose (astrocytes) and NB-B27 containing 30 mmol/L glucose (neurons). Fetal calf serum present in glial cultures contains 240 μmol/L lactate and 367 μmol/L pyruvate. To reproduce the conditions, the same concentration of lactate and pyruvate were added in neuronal cultures. At the end of the experiments, the glucose, lactate, and pyruvate concentrations in the media were determined by using kits from Boehringer (glucose), BioVision (lactate), and INstruchemie BV (pyruvate). The consumption of glucose, pyruvate, and net formation of lactate by the cells was calculated on the basis of cellular protein. Results are mean ± s.e.m. ($n=6$) of three independent experiments. Data were statistically evaluated by one-way analysis of variance followed by Student's *t*-test. Comparisons between control and *Aralar*-deficient cultures were significant where indicated ***$P\leqslant0.001$; *$P\leqslant0.05$.

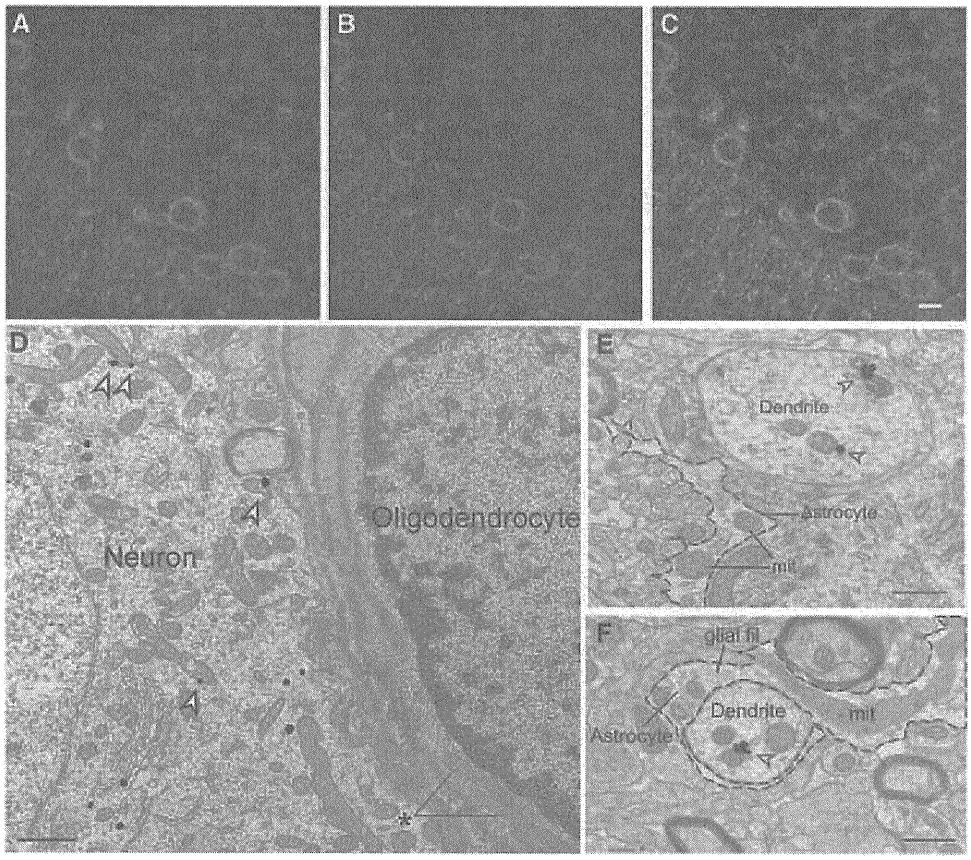

Figure 1 Aralar immunolabeling in brain neurons and astrocytes. (**A–C**) Brain sections of *Aralar*$^{+/+}$ mice (**A–C**) were probed against Aralar (green) (**A**) and Cox-I (red) (**B**) antibodies. Merged images are shown in (**C**), with nucleus marked with Topro-3 (blue). Scale bar, 10 μm. Electron microscopy analysis of Aralar immunolabeling in brain sections (**D–F**). (**D**) Prominent mitochondrial Aralar-immunogold (arrowheads) labeling in a neuronal somata, showing also some cytoplasmic gold particles. The neuron is adjacent to a glial cell (oligodendrocyte), showing the typical heterocromatic nucleus and electrodense cytoplasm, in which no Aralar immunolabeling is observed. Note the lack of labeling in the two large glial mitochondria (asterisk). Scale bar, 0.5 μm. (**E**) Arrowheads indicate Aralar-immunogold labeling on mitochondria within a dendrite. Where indicated (mit) two large unlabeled mitochondria appear in an astrocytic process (with an irregular contour marked with a dashed line), in the neuropil close to the Aralar-immunolabeled dendrite. Scale bar, 0.5 μm. (**F**) An astrocyte process showing several unlabeled mitochondria ensheathes a neuronal dendrite with one labeled mitochondria (arrowhead). The astrocyte shows a typical irregular sinuous contour and glial filaments (glial fil). Scale bar, 0.5 μm. Immunogold particles were counted in 220 electron micrographs at $\times$ 50,000 from 22 vibratome sections from five different mice. The number of particles counted in mitochondria or other regions was 731 or 210 in neurons, and 43 or 29 in glia, respectively.

(77.7%; $P = 0.0001$) and some labeling of membranes of smooth endoplasmic reticulum and intracytoplasmic tubulovesicles. The proportion of Aralar-immunogold particles localized in mitochondria in glial cells (40.3%) was statistically much lower than in neurons (two-way analysis of variance in the interaction for the two factors; type of profile and subcellular localization; $P = 0.0001$). These results indicate that, at the protein level, Aralar is localized preferentially, if not exclusively, in neurons.

Changes in Amino-Acid Levels in Brain from *Aralar*-KO Mice

As previously observed (Jalil *et al*, 2005), there is a dramatic fall in aspartate levels in brain from *Aralar*-KO mice at 20 days of age (Table 3). Other amino acids, particularly glutamate, undergo only a modest decrease (of about 25%). Essential amino acids, such as isoleucine, leucine, and lysine do not decrease. However, there is a striking decrease in serine (to 25%) and alanine (to 32%) levels and also a prominent fall in glutamine levels to about 23% in the brain of *Aralar*-KO mice.

The decrease in serine may be due to its increased utilization for pyruvate synthesis, as the pyruvate-to-lactate ratio falls drastically in neuronal cultures from *Aralar*$^{(-/-)}$ mice (Table 2). The drop in pyruvate levels may also explain the decrease in alanine, which is observed both in brain and in cultured neurons from *Aralar*-KO mice (Tables 1 and 3; Supplementary Discussion).

Table 3 Amino-acid content in brain extracts from wild-type and *Aralar*-KO mice at 20 days of postnatal age

Brain amino acids	*Wild type (nmol/g tissue)*	*Aralar-KO (nmol/g tissue) (% versus WT)*
Phosphoserine	431 ± 20	540 ± 39*
Aspartate	3006 ± 279	429 ± 108*** **(14%)**
Threonine	388 ± 20	340 ± 9
Serine	1242 ± 69	314 ± 33*** **(25%)**
Glutamate	9335 ± 815	7024 ± 455* **(75%)**
Glutamine	3806 ± 340	890 ± 167*** **(23%)**
Glycine	1863 ± 219	1563 ± 174
Alanine	755 ± 100	244 ± 22*** **(32%)**
Valine	123 ± 5	126 ± 24
Isoleucine	50 ± 2	45 ± 9
Leucine	76 ± 3	86 ± 13.1
Lysine	501 ± 51	413 ± 33
GABA	1358 ± 141	1324 ± 207

GABA, γ-aminobutyric acid; WT, wild type.
Data are expressed as nmol/g tissue (mean ± s.e.m.; $n = 6$–10). Statistical comparisons were performed using one-way analysis of variance followed by *post hoc* Duncan/Tukey *t*-test. ***$P \leqslant 0.001$; *$P \leqslant 0.05$.

No Changes in Neuronal Glutamate Levels or Synaptosomal Glutamate Release in *Aralar*-KO Mice

Cultured neurons from *Aralar*-KO mice did not show any difference in glutamate content, either when derived from cortical (Table 1) or cerebellar cultures (5.17 ± 0.21 and 5.34 ± 0.11 nmol/10^6 cells in *Aralar*$^{(+/+)}$ and *Aralar*$^{(-/-)}$ neurons, respectively (mean ± s.e.m.; $n = 4$ to 7).

We next evaluated the glutamate release and content in synaptosomes from *Aralar*-KO mice. There were no significant differences between genotypes (Supplementary Figure 3) in terms of rate of release, either in basal conditions (low K^+, with EGTA or Ca^{2+}), or after KCl stimulation (high K^+, with EGTA or Ca^{2+}). In addition, there were no differences in total glutamate content between genotypes (241.3 ± 31 and 230 ± 43 nmol glutamate/mg protein, mean ± s.e.m. of three experiments performed in triplicate, in synaptosomes from *Aralar*$^{(+/+)}$ and *Aralar*$^{(-/-)}$ mice, respectively). These results contrast with previous proposals (Palaiologos *et al*, 1988) involving the malate-aspartate shuttle in the formation of neurotransmitter glutamate (see Supplementary Discussion).

No Changes in Glutamine Utilization by Neurons from *Aralar*-KO Mice

Having shown that neuronal glutamate content and synaptosomal glutamate levels or release do not change in *Aralar*-KO, we studied whether glutamine metabolism was changed in neurons from *Aralar*-KO mice. Glutamine is deamidated to glutamate by phosphate-activated glutaminase and glutamate may be oxidized (glutamate dehydrogenase (GDH)) or transaminated (mitochondrial aspartate aminotransferase) into α-ketoglutarate (α-KG) which is subsequently decarboxylated by α-KG dehydrogenase (α-KGDH). None of these activities (phosphate-activated glutaminase, GDH, and mitochondrial aspartate aminotransferase) changed in the brain of the *Aralar*-KO mice except for an increase in α-KGDH activity (Supplementary Table 1). Cortical or cerebellar neurons from *Aralar*$^{(-/-)}$ mice did not show any changes in CO_2 production from glutamine (glutamine-derived CO_2 production 6.8 ± 0.8 and 16.3 ± 0.8 nmol Gln/mg protein/h (*Aralar*$^{+/+}$ neurons) and 8.4 ± 0.1 and 14.2 ± 01 nmol Gln/mg/h (*Aralar*$^{-/-}$ neurons) from cortex and cerebellum, respectively (mean ± s.e.m., $n = 6$)). This is consistent with the lack of effect of AST inhibitor aminooxyacetate on CO_2 production from glutamine in synaptosomes (McKenna *et al*, 1993). Thus, decreased glutamine levels in brain from *Aralar*-KO mice are not due to a change in neuronal metabolism of glutamine.

In Vivo Labeling of Cerebral Glutamine and Glutamate with ($^{13}C_2$) Acetate or (1-^{13}C) Glucose

To analyze other possible causes for the reduced glutamine levels in *Aralar*-KO brain, we investigated glutamate–glutamine synthesis *in vivo* from ($^{13}C_2$) acetate or (1-^{13}C) glucose. Figure 2 (and Supplementary Figure 4) shows that ^{13}C-labeled glutamine in the brain from *Aralar*-KO mice is below detection limit, regardless of whether ^{13}C-acetate or ^{13}C-glucose are used as cerebral substrates. The ^{13}C enrichments found in glutamate or glutamine in the control mice are similar to those observed previously (Rodrigues *et al*, 2007). However, the absence of ^{13}C-labeled glutamine in the *Aralar* $^{-/-}$ mice is unique to these animals, revealing that neuronal deprivation of Aralar results in a net decrease in astroglial synthesis of glutamine.

Decreased labeling of cerebral glutamine in the face of a very modest decrease in the cerebral glutamate pool strongly suggests that it is the astroglial synthesis of glutamine and the small astroglial glutamate pool from which it derives, which are affected. The extremely small size of the glial glutamate pool does not allow to detect changes in the labeling from ^{13}C-glucose of this pool, which is masked by the large total cerebral glutamate pool (Chapa *et al*, 2000). The absence of changes in glutamate labeling from ^{13}C-acetate can be explained by residual acetate metabolism in neurons, as the plasma acetate concentrations used in this study were well above the limit for the glial acetate transporter (Waniewski and Martin, 1998) and agrees with the lack of changes in glutamate levels in *Aralar*-deficient neurons or synaptosomes (Table 1; Supplementary Figure 3) and with the absence of changes in glutamine metabolism in Aralar-deficient neurons. As glutamine synthetase activity is unchanged in *Aralar*-KO mouse brain (Supplementary Table 1), the failure to synthesize glutamine in astrocytes must be due to a metabolic limitation in the synthesis of glutamate in brain astrocytes.